The Cooling-Canal System at the FPL Turkey Point Power Station

By David A. Chin, Ph.D., P.E., D.WRE, BCEE
Professor of Civil and Environmental Engineering
University of Miami

Executive Summary

This report was prepared under an agreement between Miami-Dade County and the University of Miami. The following issues related to the operation of the cooling-canal system (CCS) at the Turkey Point Power Station were investigated: (1) temperature variations in the CCS and associated impacts on the surrounding groundwater, (2) salinity variations in the CCS and associated impacts on the surrounding groundwater, and (3) the effects of pumping up to 100 million gallons per day from the L-31E Canal into the CCS. The principal findings of this investigation are summarized below, with analytical details supporting the findings contained in the body of the report. Data for this study was provided by the Miami-Dade County Department of Regulatory and Economic Resources. CCS temperature and salinity data for the four-year interval of 9/1/10 – 12/7/14 were made available for this investigation.

Temperature in the CCS. A heat-balance model was developed to simulate the temperature dynamics in the CCS. The results derived from the heat-balance model showed that there were two distinct periods during which the heat-rejection rate from the power plant remained approximately constant. The first period corresponded to pre-uprate conditions, and the second period corresponded to post-uprate conditions. The heat-rejection rate during the second period was found to be significantly greater than the heat-rejection rate during the first period. As a result of the increased heat addition to the CCS, the average temperature of water in the CCS has increased, and in the vicinity of the power-plant intake the average temperature has increased by approximately 2.6°C (4.7°F). This measured increase in average temperature within the intake zone is slightly greater than the increase in the maximum allowable operating temperature at the intake location of 2.2°C (4.0°F) that was approved by the Nuclear Regulatory Commission in 2014. Therefore, the increased maximum operating temperature has not reduced the probability of the intake temperatures exceeding the threshold value, which currently stands at 104°F. Since supplementary cooling of the CCS was needed in 2014, this serves as a cautionary note regarding further increases in power generation beyond 2014 levels without providing a reliable supplementary cooling system. Measured temperature data during the period of record indicate that the thermal efficiency of the CCS has decreased between the pre-uprate and post-uprate periods. Further investigation is recommended to confirm the decrease in thermal efficiency of the CCS and identify the causative factor(s). The assertion that higher algae concentrations in the CCS were responsible for the elevated temperatures in the CCS was investigated. A sensitivity analysis indicates that increased algae concentrations were not likely to have been responsible for the significantly elevated temperatures in the CCS recorded in the mid-summer months of 2014. The additional heating rate in the CCS caused by the presence of high concentrations of algae is estimated to be less than 7% of the heat-rejection rate of the power plant, hence the minimal impact. Further development of the heat-balance model is needed, since the design of any engineered system to control temperatures in the CCS must be done in tandem with heat-balance-model simulations.

Temperature impact on groundwater. Measured groundwater temperatures in some monitoring wells between the CCS and the L-31E Canal have shown higher temperatures than groundwater west of the L-31E

Canal, and this occurrence can be partially attributed to limited cooling-canal water intrusion into the Biscayne Aquifer. Monitoring-well measurements further show that nearly all of the seasonal temperature fluctuations in the groundwater occur above an elevation of -25 ft NGVD* (about 30 ft below the ground surface). At lower elevations in the aquifer, the groundwater temperature generally remains relatively steady and in the range of 75°F – 77°F (24°C – 25°C). Seasonal temperature fluctuations above -25 ft NGVD can be partially attributed to the heating and cooling of water in the L-31E Canal in response to seasonal changes in atmospheric conditions. Overall, the impact of CCS water on the temperature of groundwater in the Biscayne Aquifer can be considered as localized of not having any significant environmental consequence.

Salinity in the CCS. There has been a steady increase in CCS salinity of around 5‰ per decade since the CCS began operation in 1973. Recent measurements indicate that the rate of change of salinity might be increasing. Analyses of the salinity dynamics in the CCS were performed using a salinity model previously developed by a FPL contractor. Results from this salinity model show that evaporation and rainfall are the primary drivers affecting the salinity in the CCS, with pumpage from the interceptor ditch and blowdown from the Unit 5 generating facility also having an effect. Over prolonged periods with no rainfall, the salinity in the CCS will generally increase as fresh water is evaporated and the evaporated fresh water is replaced by saline water from the surrounding aquifer. A prolonged period with no rainfall was the primary cause for the unusually high salinities (greater than 90‰) that were observed in early summer of 2014. Seepage inflow to the CCS is mostly from the east (i.e., the area adjacent to Biscayne Bay) and seepage outflow of more saline water occurs primarily through the bottom of the CCS, thereby contributing to an increased salinity of the underlying groundwater. The short-term (seasonal) salinity fluctuations in the CCS are controlled by seasonal variations in the amount and timing of rainfall, and aperiodic spikes in salinity should be considered as being normal and expected. In the long term, barring any significant intervention, salinities will continue to follow an upward trend, since over the long term annual evaporation exceeds annual rainfall. Increased temperatures in the CCS lead to increased evaporation which increases the rate of change of salinity in the CCS above historical rates of change. The steady increase in salinity could be mitigated by an engineered system to add supplemental water with lesser salinity. However, pumping lower salinity water into the CCS in large quantities will elevate the water level in the CCS, decrease the seaward piezometric-head gradient, and likely exacerbate the inland intrusion of saltwater originating from the CCS. The effectiveness of an engineered system that pumps saline water from the CCS to deep-well(s) for disposal will depend on the groundwater-flow response in the aquifer surrounding the CCS, the induced salinity-transport dynamics within the aquifer, and the operational protocol of the deep-well injection system. Data in support of such a proposed system was not made available to the investigator during this study.

Salinity impact on groundwater. Based on available documentation and data summaries contained in numerous reports prepared by FPL, SFWMD, and DERM, there is little doubt that seepage from the CCS into the Biscayne Aquifer has caused salinity increases within the aquifer, and this impact extends several miles inland from the CCS. The strongest evidence for this assertion comes from the analysis of tritium data. The CCS contains water with a high tritium concentration, and utilization of tritium as a tracer to identify groundwater originating from the CCS is justified. Elevated concentrations of tritium above a 20 pCi/L threshold in the deep groundwater can reasonably be attributed to the presence of water originating from the CCS. The approximate limit of the 20 pCi/L concentration contour has been reported to be 3.8 – 4.7 miles west of the CCS and 2.1 miles east of the CCS.

*"NGVD" refers to the NGVD 29 datum.

Withdrawal of 100 mgd from the L-31E Canal. Adverse impacts of pumping 100 mgd from the L-31E Canal into the CCS during June 1 – November 30 are likely to occur under the current permitted pumping protocol. Under the current pumping protocol stipulated in the SFWMD-issued permit, the stage in the L-31E Canal will be held constant during pumping, while the stage in the CCS will generally rise as a result of pumping. This combined effect will decrease, or possibly reverse, the seaward piezometric-head gradient between the L-31E Canal and the CCS that would normally exist in the absence of pumping. A possible consequence of a reversed head gradient between the L-31E Canal and the CCS is advection of a saline plume from the CCS towards the L-31E Canal, and creation of a circulation cell in which the salinity of the water in the L-31E Canal is increased as the saline plume enters the L-31E Canal. Furthermore, according to model results provided by FPL in support of the pumping-permit application, pumping of 100 mgd into the CCS is likely to reduce the water-level differential between the L-31E Canal and the CCS to below the 0.30 ft threshold that would normally trigger the operation of the interceptor ditch salinity-control system, which, if operational, would further reduce the head gradient between the L-31E Canal and the CCS. Based on these findings, it is recommended that the permitted pumping protocol be revised prior to the 2016 pumping period. The revised protocol should include, as a minimum, real-time monitoring of the stages in the CCS and the L-31E Canal during pumping operations, specification of a threshold water-level difference between the L-31E Canal and the CCS that would limit further pumping, and real-time monitoring of the salinity in the L-31E Canal during pumping operations.

Recommended actions. The following specific action items would lead to better and more efficient management of the cooling-canal system:

- Develop a calibrated heat-balance model to simulate the thermal dynamics in the CCS, and collect the data necessary to calibrate and validate this model.
- Confirm and identify the causative factors for the decline in the thermal efficiency of the CCS between the pre-uprate and post-uprate periods.
- Develop a quantitative relationship for estimating algae concentrations in the CCS as a function of temperature, salinity, and nutrient levels.
- Develop a locally validated relationship between the evaporation rate, water temperature, air temperature, wind speed, salinity, and algae concentrations in the CCS.
- Modify the operational protocol associated with the 2015 – 2016 permit for transferring up to 100 mgd from the L-31E Canal to the CCS.

The analyses and recommendations contained in this report are offered in support of the goal of achieving an environmental balance for the sustainable generation of electrical power at the Turkey Point power station.

(This page is intentionally left blank.)

Contents

1 Background

This investigation is primarily focused on the operation of the cooling-canal system (CCS) located at the Turkey Point power-generating station in south Miami-Dade County, Florida. The issues of concern relate primarily to the increased temperatures and salinities that have recently been measured in the CCS, the environmental impacts of these increased levels on the quality of groundwater in the Biscayne Aquifer, the need for additional engineered systems to supply supplemental cooling water to the CCS, and the environmental impacts of permitted pumping of up to 100 mgd of water from the L-31E Canal to the CCS between June 1 and November 30.

Environmental concerns. Most of the environmental concerns regarding the operation of the cooling-canal system (CCS) at Turkey Point relate to: (1) the sustainability of the system in maintaining adequate temperatures to cool the power-generating units, (2) the impact that current and projected future salinities in the CCS have on the quality of groundwater in the surrounding Biscayne Aquifer, and (3) the need for new supplementary sources of water and/or revised operational protocols to control the temperatures and salinities in the CCS. Specific issues of concern are as follows:

- Increased temperatures in the CCS limit the effectiveness of the CCS as a cooling-water source servicing four power-generating units. When the intake temperature in the CCS exceeds a regulatory limiting value of 104°F, either power generation must be curtailed or supplementary cooling water must be provided to the CCS to reduce the temperature and hence keep the generating units in operation; the sustainability of a supplementary system to cool the water in the CCS has not yet been established.

- Increased salinity in the CCS likely contributes to increased saltwater intrusion within the Biscayne Aquifer, thereby deteriorating the groundwater quality underlying inland areas. The current salinity-control system, sometimes called the interceptor-ditch system, has not been effective in controlling the inland migration of saline water from the CCS, thereby signaling the need for revised operating strategies to manage salinity intrusion resulting from CCS operation.

- The effectiveness of the permitted protocol for pumping 100 mgd from the L-31E Canal into the CCS to reduce temperatures in the CCS, and the effect of this pumping operation on saltwater intrusion in the Biscayne Aquifer and water quality within the L-31E Canal are issues that are yet to be resolved.

This report summarizes what is currently known about the CCS, summarizes key findings from previous related investigations, regulatory reports and reviews, provides new analyses, and gives suggested answers and pathways forward to resolve several issues related to the above-listed concerns.

1.1 Turkey Point Power Station

The Turkey Point Power Station currently consists of five power-generating units: two 404-MW oil/natural gas-fired generating units (Units 1 and 2), two 728-MW nuclear-powered units (Units 3 and 4), and a nominal 1150-MW natural gas-fired combined-cycle unit (Unit 5). In 2002, the Nuclear Regulatory Commission (NRC) extended the operating licenses for both nuclear reactors from forty years to sixty years, extending licensed operation to the year 2033. In June of 2009 the Florida Department of Environmental Protection (FDEP) issued certification for the increase in power-generating capacity (commonly called an “uprate”) of

Units 3 and 4 to provide an additional 250 MW of power. Unit 3 has been operating at its uprated power-generation capacity since Nov 2012, and Unit 4 has been operated at its uprated power-generation capacity since May 2013. In planning for the Unit 3 and Unit 4 uprates, it was anticipated that the uprate would increase the temperature of the cooling water discharged to the CCS by 2.5°F (1.4°C), from 106.1°F to 108.6°F (41.2°C to 42.6°C) (FPL 2011), and that the increased temperature in the CCS might result in increased evaporation and increased salinity. The CCS provides cooling water for Units 1 to 4, with cooling of Unit 5 accomplished by mechanical-draft cooling towers that use make-up water drawn from the Upper Floridan Aquifer. Blowdown water from Unit 5 is discharged into the CCS. Since the uprate of Units 3 and 4 went into effect, Unit 2 has not been operational. In 2014, the Florida legislature approved construction of two additional nuclear reactors at Turkey Point (Units 6 and 7), with each additional unit having an approximate electrical output of 1100 MW; approval of the additional units by the NRC is currently pending. The two additional nuclear reactors will not use the CCS for cooling. Presently, with an estimated total power-station capacity of approximately 3550 MW, the Turkey Point power station is the second largest power station in Florida, in terms of generating capacity, and is the sixth largest power station in the United States (NRC, 2012).

1.2 Geohydrology

The Turkey Point power station and associated cooling-canal system (CCS) are underlain by the Biscayne Aquifer. In the vicinity of Turkey Point, the Biscayne Aquifer extends from land surface to a depth of approximately 106 ft below sea level (BSL), with the thickness of the aquifer decreasing towards the west. Geologic formations within the Biscayne Aquifer include, from the ground surface downward, the Miami Limestone Formation, Key Largo/Fort Thompson Formations, and upper portions of the Tamiami Formation. The less-permeable units of the Tamiami Formation, and the deeper Hawthorn Group, form the confining unit between the Biscayne Aquifer and the Upper Floridan aquifer. The top of the confining unit is characterized by the transition between highly permeable beds of the Fort Thompson Formation and the lower-permeability silty sands of the Tamiami Formation. The thickness of the Miami Limestone Formation is in the range of 8 – 23 ft, and the thickness of the Fort Thompson Formation is in the range of 46 – 95 ft. The regional groundwater flow direction is, on average, from the northwest to southeast (Fish and Stewart 1991), although the predominant flow direction at the coast can vary significantly between the wet and dry seasons. The water-table gradient is typically towards the coast during the wet season (May – October), but can be directed inland during the dry season (October – April). The possibility of the occurrence of an inland water-table gradient is the primary reason for the so-called "interceptor-ditch system" that is used ostensibly to control the inland migration of saline water originating from the CCS. Water-table elevations at Turkey Point are typically around 1 ft NGVD, and the magnitude of the average regional water-table gradient is typically in the range of 0.004% – 0.005%. Notably, with such small water-table gradients, small errors in measured water-table elevations can significantly impact the accuracy of the estimated gradients. Vertical piezometric-head gradients at the Turkey Point site (away from the CCS) are typically negligible, with piezometric-head differentials between shallow, intermediate, and deep zones reportedly being within hundredths of a foot.

Groundwater classification. Groundwater at the Turkey Point site was originally classified by FDEP as as G-II, which is the classification for groundwater that is of possible potable use and has a total dissolved solids content of less than 10,000 mg/L. In September 1983, at the request of FPL, the groundwater at the Turkey Point site was reclassified by FDEP as G-III, which is the classification for groundwater that

has a total dissolved solids content of 10,000 mg/L or greater, or has a total dissolved solids of 3,000 – 10,000 mg/L and has no reasonable potential as a future source of drinking water. The G-III classification currently remains in effect.

1.3 The Cooling-Canal System

History and regulation. Construction of the cooling-canal system (CCS) was approved by the Dade County Board of County Commissioners in November 1971, and became operational in February 1973. At the time of its initial operation, the CCS was approximately half-way completed compared with the present system. The CCS is sometimes referred to as an Industrial Wastewater Facility (IWW) since the circulating water system, which discharges saline water to the surrounding aquifer, is regulated under the federal National Pollutant Discharge Elimination System (NPDES) and an Industrial Wastewater (IW) permit issued to FPL by the Florida Department of Environmental Protection.

Current canal system. In its present state, the CCS is approximately two miles wide (east–west) and five miles long (north–south), covers an area of approximately 5900 acres, and has approximately 4370 acres of water surface. The CCS consists of 32 canals flowing south from the discharge location in the north, and 7 return canals flowing north to the intake location. Because the south-flowing canals are located in the western section of the CCS and the north-flowing canals are located in the eastern section of the CCS, the system is sometimes referred to as having 32 western canals and 7 eastern canals. The south-flowing (western) canals are each approximately 4 ft deep, 200 ft wide, and spaced approximately 90 ft apart; these canals range in length from 2 – 5 miles. The 4 ft depth of the canals (from ground surface) was originally chosen so as to not penetrate the less-permeable surficial Miami Oolite Formation that extends to about 4 ft below grade, thereby minimizing groundwater exchange between the CCS and the underlying Biscayne Aquifer. The bottom of the canals are below the lowest water-table elevation expected in the Biscayne Aquifer at Turkey Point, and therefore the canals always contain water that is directly connected to the adjacent groundwater. Cooling water leaves the four generating units (Units 1 – 4), flows into Lake Warren, and then into the 20-ft deep 100-ft wide feeder canal that connects to the 32 south-flowing cooling canals. Four shallow cross canals spaced 1-mile apart run east – west across the 32 south-flowing cooling canals. These cross canals contain flow-control structures that distribute water flow evenly to the canals so that each cooling canal carries a flow that is proportional to its surface area in order to optimize heat exchange with the atmosphere. At the southern end of the CCS is a collector canal that is approximately 20 ft deep and 200 ft wide. Water returns to the power-generating units from the southern collector canal via 6 north-flowing canals, the largest of which is the Card Sound Canal which is 200 ft wide and 20 ft deep. The average length of the circulation path between the discharge and intake locations is 13.4 miles. The 32 south-flowing cooling canals are numbered from 1 to 32, from east to west, hence, cooling-canal number 32 is the westernmost canal in the CCS. Endangered American crocodiles (*Crocodylus acutus*) inhabit the cooling canals. During nesting season, more than 40 adult crocodiles have been observed in the canals, although there have been some reports that the crocodile population in the CCS is declining possibly due directly or indirectly to the increased salinities in the CCS.

Operational characteristics. The canals in the CCS were designed to operate at a total flow rate of 4250 ft^3/s (2750 mgd) when all four generating units (Units 1 – 4) supported by the CCS are in full operation. Small wastewater (blowdown) flows from Unit 5 are also discharged into the CCS. Typically, the flow rate through the CCS varies significantly with the electric load demand on the generating units, and is

usually in the range of 2700 – 4250 ft^3/s (1750 – 2750 mgd) on any given day, with a typical flow depth of around 2.8 ft. Thermal energy is dissipated in CCS as water moves from north to south, with the primary heat-exchange processes being evaporation, solar radiation, and both emitted and absorbed longwave radiation. Maximum temperatures near the discharge location of the power-generating units are typically around 108°F (42°C), and maximum temperatures near intake to the power-generating units are typically around 93°F (34°C); the difference between these typical maxima is 15°F (8°C), which gives a measure of the cooling effect of the CCS. The (regulated) maximum allowable temperature at the intake location in the CCS is 104°F (40°C). The flow in the CCS is driven by 12 condenser-circulating pumps and auxiliary cooling pumps. The CCS typically contains approximately 7×10^8 ft^3 of water, and the average velocity is around 0.25 ft/s in each canal. Approximately two days (44 – 48 h) are required for water in the CCS to travel from the discharge location to the intake location. Within the CCS, the flow is maintained by a head differential between the discharge and intake locations, with the water-surface elevation being highest at the discharge location and lowest at the intake location. The water level at the discharge location is typically about 3 ft higher than the water level at the intake location. Typical water surface elevations in the CCS are 2.04 ft NGVD at the discharge location, 0.76 ft NGVD at the south end, and -0.77 ft NGVD at the intake location. The water-surface elevation at south end of the CCS is usually closest to the water-surface elevation in Biscayne Bay. The water-surface elevation in the CCS is typically higher than the site-average water-table elevation in the Biscayne Aquifer at the discharge (north) end of the system, approximately equal to the water-table elevation at the south end of the system, and below the water table at the intake (north) end of the system. Consequently, water generally flows out of the CCS into the aquifer near the discharge location of the CCS and water generally flows into the CCS from the aquifer near the intake location of the CCS, there is less flow interaction between the CCS and the aquifer at the southern end of the system. During very heavy rains, there can be a net inflow to the CCS from the surrounding aquifer. The CCS is approximately nontidal, and water in the CCS is typically warmer than the air temperature. The effectiveness of the CCS as a cooling system decreases as the temperature in the CCS increases.

1.4 Algae in the CCS

A significant algae bloom occurred in the CCS during 2014 and algae in now perceived to be a problem in the CCS. Prior to 2013, only limited and short-term algae blooms had occurred in the CCS, typically during the early summer months. In fact, algae blooms were of such limited concern that routine monitoring for algae was not commonly done prior to 2014. In the summer of 2014, large-scale application of a $CuSO_4$-based algaecide was used to reduce the algae concentrations in the CCS. The applied algaecide was reported as being ineffective in reducing the algae concentrations, serving only to stabilize the existing concentrations (SFWMD, 2015).

Factors affecting algae concentrations. High concentrations of algae have been observed in the CCS with correspondingly high concentrations of nutrients being measured. The historical average algae concentration in the CCS is reported to be 50 cell/L[†], however, in the summer of 2014 algae concentrations as high as 1600 cell/L were reported (SFWMD, 2015). The addition of nutrients from the power-generating units into the CCS is assumed to be negligible, with nutrients likely originating from allochthonous sources. Total nitrogen (TN) concentrations in the CCS have been reported in the range of 1.7 – 5.3 mg/L (Ecology and Environment, Inc., 2012). The highest reported TN concentrations in the CCS were measured at all stations in March 2012, which coincided with higher turbidities and pH in the CCS. The majority of the nitrogen

[†]Algae concentrations are normally given in Chl*a*/L, so these units are unusual.

in the CCS appears to be in organic form (typically 80% – 90%). Total phosphorus (TP) concentrations in the CCS have been reported in the range of 4 – 73 μg/L, with an overall average concentration of 36 μg/L. Numerous measurements of TN and TP have been reported between 7/2010 and 3/2015 (Ecology and Environment, Inc., 2010; 2011a; 2011b; 2012a; 2012b; 2012c; 2013a; 2013b; 2014a; 2014b; 2015), and synoptic measurements within this time period yield TN/TP values in the range of 48 – 2015 with a median value of 142. Since the measured TN/TP values generally exceed the Redfield ratio of 16, it can be inferred that TP is the controlling nutrient for algae growth in the CCS. The existence of TP control of algae growth in saline systems is commonly attributed to the presence of nitrogen-fixing planktonic cyanobacteria which make up any short-term nitrogen deficits (Howarth and Marino, 2006). It has been reported that the cyanobacteria *Aphanothece* sp. are the predominant algae species in the CCS; these species are nitrogen-fixing and thrive under hypersaline conditions. In addition to nutrients, both temperature and salinity are known to affect the growth of algae in water bodies. For given nutrient levels, increasing temperatures usually contribute to increased algae concentrations, and increasing salinities usually contribute to decreased algae concentrations (Håkanson and Eklund, 2010). However, for the algae species commonly found within the CCS, algae concentrations have been reported to increase with increasing salinity (SFWMD, 2015). Algae concentrations are usually expressed in terms of the mass of chlorophyll-a per liter. Synoptic measurements of chlorophyll-a (Chl$a$) concentration, salinity (S), temperature (T), and total phosphorus (TP) concentration at locations near the discharge and intake locations in the CCS between May 31, 2015 and November 13, 2015 are plotted in Figure 1. These synoptic measurements collectively show the algae concentration

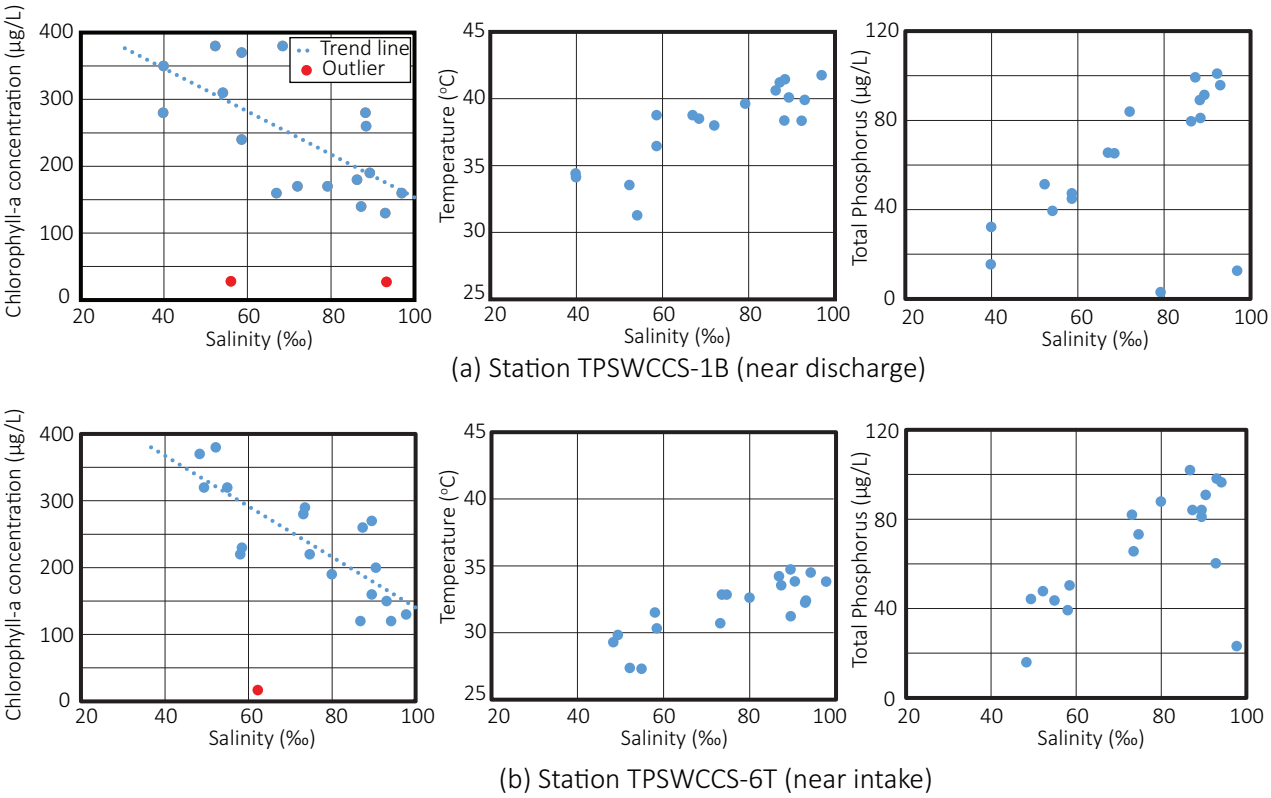

Figure 1: Chlorophyll-a levels in the CCS as a function of temperature, salinity, and total phosphorus

(Chl$a$) decreasing with increasing salinity (S), decreasing with increasing temperature (T), and decreasing

with increasing nutrient concentration (TP). All of these trends are contrary to the natural relationships between Chl$a$, S, T, and TP and are either anomalous or indicate the effect of an algaecide. Assuming that a $CuSO_4$-based algaecide was applied during the period of measurements, the effectiveness of the algaecide can be seen by plotting the relationship between Chl$a$ and sulfate (SO_4) concentrations, and this relationship is shown in Figure 2. It is apparent from Figure 2 that algae concentrations decrease significantly with

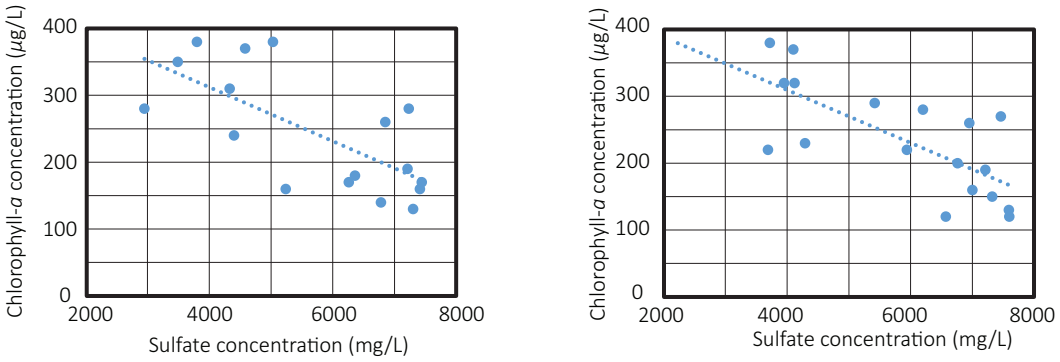

(a) Station TPSWCCS-1B (near discharge) (b) Station TPSWCCS-6T (near intake)

Figure 2: Chlorophyll-a levels in the CCS sulfate concentrations

increasing concentrations of algaecide (as measured by sulfate concentration), indicating that addition of an algaecide is an effective means of reducing algae concentrations in the CCS. However, it should also be kept in mind that Chl$a$ reductions caused by an algaecide are necessarily only temporary, since the natural factors causing high levels of Chl$a$ (i.e., S, T, and TP) remain at elevated levels within the CCS. Since the system is autotrophic, reduction of autochthonous TP levels should be targeted to ultimately reduce both algae levels and the need for repeated application of algaecide(s) in the CCS.

Impact of increased algae concentrations. It has been asserted (SFWMD, 2015) that increased algae concentrations and turbidities associated with algae blooms cause more solar energy to be absorbed in the CCS, and reduces the ability of the CCS to dissipate thermal energy. The primary mechanisms by which the CCS dissipates thermal energy are by evaporation and the emission of longwave radiation. A conventional assumption made by engineers and scientists is that the evaporation rate from a water body is unaffected by the concentration of algae in the water body. There is no scientific evidence documented in any published studies showing that the rate of evaporation from a water body is reduced by high algae concentrations. Further, there are no published studies showing that the emission of longwave radiation from a water body is particularly sensitive to the concentration of algae in the water. As a consequence, the primary effect of increased algae concentrations in the CCS can be assumed to be increased absorption of solar radiation, which would increase the heating of the water and elevate the temperature of the water in the CCS. The quantitative effect of increased solar heating of the CCS due to increased algae concentrations is parameterized by a reduced albedo of the water surface, and the relationship between the reduced albedo and the corresponding increased temperature was investigated in this study using a heat-balance model described subsequently in Section 2.2 of this report. It should be noted that the "trapping" of solar energy due to increased algae concentrations would be moderated by the resulting increased evaporation which would cause increased cooling due to the extraction of the latent heat of vaporization.

1.5 Saltwater Intrusion

The inland extent of saltwater intrusion in the Biscayne Aquifer is defined by the location of the 1000 mg/L isochlor. As a reference concentration, the South Florida Water Management District (SFWMD) defines seawater as having a chlorinity (i.e., chloride concentration) greater than 19,000 mg/L, and saline water as having a chlorinity greater than 250 mg/L. Surface waters with chlorinities greater than 1500 mg/L are classified as marine waters, and surface waters with chlorinities less than 1500 mg/L are classified as fresh waters (F.A.C. 62-302.200). The landward extent of the saltwater interface (i.e., the 1000 mg/L isochlor) varies naturally in response to a variety of factors, such as seasonal variations groundwater recharge and variations in rates at which groundwater is pumped from the aquifer. For example, prolonged droughts or excessive water usage inland that reduce water-table elevations can cause increased salinity intrusion. Prior to the construction of the CCS, the groundwater underlying the Turkey Point site was naturally saline due to the proximity of the site to the coast. In fact, had the groundwater not been saline, construction of the cooling-canal system at Turkey Point would not have been permitted. Since the water-table gradient towards the coast at Turkey Point is typically very low, and with the location of the saltwater interface being partially controlled by those gradients, even slight reductions of the fresh water piezometric-head gradient can cause substantial landward movement of the saltwater interface. The occurrence of landward gradients during the dry season promotes inland movement of saline groundwater.

CCS impact on saltwater intrusion. It has always been recognized that construction of the CCS without any mitigating salinity-control systems would cause the saltwater interface to move further inland. This expectation was based on the assertion that construction of a CCS containing saline water one mile inland from the coast is tantamount to moving the coast one mile inland, and also moving the associated saltwater wedge around one mile inland. Since water in the CCS has a higher salinity than seawater, and is therefore denser that the water in Biscayne Bay, the effect of the CCS is actually greater than moving the coast one mile inland. To compound this effect, the engineering consultants that originally analyzed the performance of the CCS also asserted that if the water level in the CCS were to be increased by 0.50 ft above the preconstruction water-table elevation, then the toe of saltwater water wedge at the base of the Biscayne Aquifer might move approximately 7.5 miles further inland during the dry season as compared to its original location during the dry season. The engineering consultants also asserted that in the wet season, an elevated water level of 0.50 ft in the CCS might move the toe of the saltwater wedge approximately 1 mile further inland compared to its original location during the wet season. Based partially on these expectations, the salinity-control system that is currently in place was designed to control the westward migration of saltwater originating in the CCS. This control system involves pumping water from a so-called “interceptor ditch” into the CCS in order to create a seaward hydraulic gradient between the L-31E Canal and the interceptor ditch, where the L-31E Canal is located to the west of the interceptor ditch. The protocol for operating this salinity-control system and the effectiveness of the system are discussed in Section 1.6 of this report.

Tracing the movement of CCS water in the Biscayne Aquifer. Tritium has been selected by the cognizant regulatory agencies (SFWMD and DERM) to trace the movement of CCS water in the Biscayne Aquifer. Historical data from 1974 to 1975 showed CCS tritium concentrations in the CCS to be in the range of 1556 – 4846 pCi/L, and reports submitted by FPL for the monitoring period from June 2010 through December 2011 showed CCS tritium concentrations in the range of 1260 – 14,280 pCi/L. Natural groundwater at the base of the Biscayne Aquifer would be expected to have relatively low concentrations of tritium. A threshold concentration of 20 pCi/L has been used as a baseline to infer the presence of groundwater orig-

inating from the CCS. Groundwater with concentrations below 20 pCi/L are presumed not to be affected by the CCS. FPL does not concur with the selection of 20 pCi/L as a threshold or background tritium concentration for surface water, pore water, or shallow groundwater. The basis of FPL's contention regarding the 20 pCi/L threshold is that multiple factors such as atmospheric deposition, vapor exchange, and errors in laboratory analysis can influence reported tritium levels. The FPL assertion is reasonable and is supported by measured data that indicate atmospheric and vapor exchange effects on tritium concentrations can be particularly significant in surface water and shallow groundwater, with significance decreasing with distance from the CCS. However, at depth, the CCS appears to be the primary source of tritium, and using tritium as a tracer in the lower elevations of the Biscayne Aquifer is reasonable. Reported measurements show groundwater tritium concentrations in excess of 3000 pCi/L near the CCS, with concentrations decreasing with distance from the CCS, and found at concentrations of hundreds of pCi/L three miles west of the CCS at depth. The approximate limit of the 20 pCi/L concentration contour is 3.8 – 4.7 mi west of the CCS and 2.1 mi east of the CCS. Based on the strength of these data and supporting analyses, it is reasonable to conclude that operation of the CCS has impacted the salinity of the Biscayne Aquifer within the limits of the 20 pCi/L contour.

1.6 L-31E Canal and Interceptor Ditch

L-31E Canal Levee L-31E and its adjacent 20-ft deep borrow canal to the west of the levee were primarily constructed as a barrier to prevent salinity intrusion to locations west of the canal. The L-31E Canal collects water from other drainage canals in the area that include Military Canal, North Canal, Florida City Canal, North Model Land Canal (C-106), and South Model Land Canal (C-107). The L-31E Canal discharges into Biscayne Bay through structures S-20 and S-20F in the vicinity of Turkey Point. The L-31E Canal was constructed in the late 1960's by the U.S. Army Corps of Engineers and the Central and Southern Florida Flood Control District (CSFFCD), where the CSFFCD was later renamed the South Florida Water Management District (SFWMD).

Interceptor ditch control system. The interceptor-ditch (ID) salinity-control system was designed to prevent the seepage of water from the CCS westward within the Biscayne Aquifer. The ID, which is located immediately to the west of the CCS, is occasionally pumped to create a seaward water-table gradient between the L-31E Canal to the west and the ID to the east, with the basis for the effectiveness of the ID control system being that groundwater originating in the CCS will be prevented from migrating towards the west in the presence of an eastward water-table gradient between the L-31E Canal and the ID. The ID is pumped when a natural seaward water-table gradient between the L-31E Canal and the ID does not exist, and usually this is needed only during the dry season (November – April). The ID is adjacent and parallel to cooling-canal number 32 (CC-32) at the western end of the CCS, and was constructed at the same time as the CCS. The ID is approximately 18 – 20 ft deep, 30 ft wide, and 29,000 ft (5.5 mi) long. Within the ID are two pump stations, with each station containing two pumps, each capable of pumping up to 15,000 gpm (21.6 mgd). There is no mechanism to transfer water between the ID and CCS, except for the 4 pumps at the two pump stations. The L-31E Canal, ID, and CC-32 are all approximately parallel to each other and run at an angle of approximately $17°38'$ west of south. The perpendicular horizontal distance between the L-31E Canal and the ID is about 1000 ft. When the ID is pumped, there is a quick and measurable response in water levels in the L-31E Canal and the monitoring wells closest to the ID, indicating that there is good connectivity between the ID, L-31E Canal, and nearby monitoring wells.

Interceptor ditch operating rule (1973 – 2011). The ID operating rule that was followed from the initial date of operation of the CCS in February 1973 up until December 2011 (i.e., for 38 years) was as follows:

- Whenever the water-surface elevation in the L-31E Canal is more than 0.2 ft higher than the water-surface elevation in CC-32, there is a seaward water-level gradient and no pumping is necessary.
- If the above criterion is not met, a seaward gradient is still taken to exist if the water-surface elevation in the L-31E Canal is more than 0.3 ft higher than the water-surface elevation in the ID. Under this condition no pumping is necessary.
- If neither of the above two criteria are met, pumping of the ID is initiated and the pumping rates are adjusted to meet the 0.3-ft water-level difference criterion between the L-31E Canal and the ID.
- Pumping is terminated when the criteria for a natural water-table gradient is met (without pumping).

Although this operating rule is no longer in effect, it is still relevant to this analysis since possible westward migration of saline water from the CCS into the Biscayne Aquifer could have occurred while following this operating rule. This concern is discussed subsequently.

Interceptor ditch operating rule (2011 – present). A more conservative revised operating rule for the ID was initiated in December 2011 that considered freshwater piezometric-head equivalents rather than measured water-table elevations. This resulted in changes to the ID operating rule, and since December 2011 the ID operating rule in effect is as follows:

- If the L-31E Canal water-surface elevation minus the CC-32 water-surface elevation is equal to or greater than 0.30 ft then no pumping of ID is necessary, and a seaward gradient exists.
- If the L-31E Canal water-surface elevation minus the CC-32 water-surface elevation is less than 0.30 ft, a natural seaward gradient might still exist if the L-31E Canal water-surface elevation minus the ID water-surface elevation is equal to or greater than 0.30 ft and the density of the water in the ID is less than or equal to 1012 kg/m^3. If a density in the ID is greater than 1012 kg/m^3, a higher elevation difference between L-31E and the ID is necessary and can be calculated by converting the surface-water levels to freshwater piezometric-head equivalents.
- If a natural seaward gradient does not exist, create an artificial seaward gradient by pumping the ID until the ID is maintained at an elevation difference of at least 0.30 – 0.70 ft between the L-31E Canal and the ID, depending on the density of the ID water.

The primary change between this revised operating rule and the previous operating rule is the increase in the L-31E/ID/CC-32 water-level difference criteria and the consideration of variable-density effects. The use of freshwater piezometric-head equivalents provides a more rigorous approach to the operation of the ID.

Effectiveness of the ID salinity-control system. Both the current and previous operating rules of the ID salinity-control system have limited salinity-control effects and do not prevent the landward migration of saline water originating from the CCS under all conditions. Following either of these operating rules, pumping of the ID reduces the water level in the ID below that in the L-31E Canal thereby creating a seaward water-table gradient and presumably precluding westward migration of groundwater originating in the CCS. However, pumping water from the ID into the CCS generally elevates the water-surface in the CCS and it is

possible for the water level in the CCS to be above the water level in the L-31E Canal, which then creates the possibility that water originating in the CCS could pass under the ID even when the pumps in the ID are running to prevent this occurrence. Interestingly, this scenario was recognized in an early report prepared by the design engineers (Dames and Moore, 1971) based on results derived from an analog model of the system. The analog model showed that westward migration of the saltwater interface is possible even if the ID operating rule is followed. Further, Golder (2008) stated that operation of the ID salinity-control system would prevent westward migration of CCS water "at least in the top 18 ft of groundwater." Measurements taken during ID pumping have in fact shown several occurrences where the water level in the CCS exceeds that in the L-31E Canal during ID pump operation, thereby indicating the possible ineffectiveness of the ID salinity-control system. In actuality, the functioning of the ID salinity-control system is more accurately characterized as intercepting shallow saline groundwater adjacent to the ID that is then pumped back to the CCS when the natural gradients are low and the potential for saltwater intrusion exists. It is possible that pumping of the ID under some circumstances simply creates a shallow subsurface (groundwater) circulation in which water from the CCS flows into the ID as groundwater that is subsequently returned to the CCS as pumped water. In support of this assertion, time series plots show that there are periods during pumping of the ID when the bottom-water temperatures in the ID rose along with an increase in specific conductance in the ID (Ecology and Environment, Inc., 2014). Aside from concerns regarding the effectiveness of the ID control system in mitigating saltwater intrusion, secondary concerns have also been raised that the ID control system contributes to the deterioration of groundwater quality in that it generally pumps less-saline water from the ID into the hypersaline CCS which further contributes to increased salinity in the aquifer.

2 Temperature Variations in the Cooling Canals

The temperature in the CCS at the intakes to the power-generating units affect the efficiency and power output of the generating units that use water from the CCS. Both the efficiency and the power output of the generating units decrease with higher cooling-water temperatures. The practical upper limit of the intake cooling-water temperature is determined by the characteristics of the condensers and auxiliary heat exchangers in the generating units. In 2014 the Nuclear Regulatory Commission granted FPL's request to increase the maximum intake cooling-water temperature from 100°F to 104°F (37.8°C to 40°C). If the intake cooling-water temperatures in the CCS were to exceed 104°F, then FPL would be required to reduce power output and possibly shut down one or more of the power-generating units. Since this occurrence would adversely affect a large number of customers in the South Florida service region, Miami-Dade County is obliged to work with FPL to find ways to avoid cutbacks in power generation resulting from elevated temperatures in the CCS.

2.1 Results from Previous Studies

2.1.1 Temperatures in the CCS

Water temperatures in the CCS are almost always higher than synoptic temperatures of the overlying air, and temperatures in the CCS are almost always higher than temperatures in nearby Biscayne Bay. Analyses done by FPL's engineering consultants in around 2008 anticipated that the uprate of Units 3 and 4 would cause a maximum temperature increase of 2.5°F (1.4°C) in the cooling water discharged to the CCS and an increase of 0.9°F (0.5°C) in the temperature of the intake water (reported in SFWMD, 2008). These temperature changes were predicted to result in an increase in evaporation from the CCS of around 2 –

3 mgd, and the increased evaporation was expected to increase the salinity in the CCS by 2‰ – 3‰. In contrast to the aforementioned predictions, it has been generally reported that temperatures in the CCS have actually increased by 5 – 9°F (3 – 5°C) in the post-uprate period compared with the pre-uprate period. In the summer of 2014 (during the post-uprate period), temperatures in the CCS were sufficiently elevated as to prompt concern regarding the sustainability of the CCS as an adequate source of cooling water to the power-generating units. According to FPL's consultant (Ecology and Environment, Inc., 2014), the increase in CCS water temperatures in the post-uprate period cannot be attributed to the uprate since the total heat rejection rate to the CCS from Units 1, 2, 3, and 4, operating at full capacity prior to the uprate would have been higher than the post-uprate heat rejection rate to the CCS for Units 1, 3, and 4, operating at full capacity. Unit 2 in the post-uprate period has been dedicated to operate in a synchronous generator mode and hence not producing steam heat.

2.1.2 Thermal Efficiency of the CCS

The thermal efficiency of the CCS is a measure of the ability of the CCS to cool the discharged water down to the background air temperature. An investigation of the thermal efficiency of the CCS was performed by Lyerly (1998), and these analyses indicated that the thermal efficiency of the CCS at the time of the study was equal to 86.4%. This efficiency was based on a 24-h average discharge temperature of 107.3°F (41.8°C), average intake temperature of 91.1°F (32.8°C), and an average air temperature of 88.6°F (31.4°C). In analyzing the temperature measurements, Lyerly (1998) noted that most of the cooling (i.e., most of the temperature decrease) occurs as the water in the CCS flows from the (north) discharge location to (south) collector canal, with much less temperature decrease as the water flows back from the collector canal to the (north) intake location. It is expected that the thermal performance varies with flow rate and the state of the CCS, so the reported thermal efficiency should be regarded more as a snapshot of conditions at the time of the measurements than as a constant value. More recent measurements between June 2010 and June 2012 (Ecology and the Environment, 2012) show water temperatures in the CCS on the discharge side of the power-generating units being around 13.5°F (7.5°C) warmer on average than at the intake side of the power-generating units. The average temperature at the south end of the CCS was only 2°F (1.1°C) warmer than at the intake side of the power-generating units, which supports the assertion that most of the cooling in the CCS occurs as the water flows from north to south.

2.1.3 Thermal Effects on Groundwater

Measured groundwater temperatures in some wells between the ID and the L-31E Canal show higher temperatures than the groundwater west of the L-31E Canal, and this occurrence has been partially attributed to limited cooling-canal water intrusion (Dames and Moore, 1977). A "groundwater thermocline" has been reported to exist in the area west of the CCS, which shows a sudden decrease in groundwater temperature at a particular depth in the aquifer. Measurements show that nearly all of the seasonal temperature fluctuations occur above an elevation of −25 ft NGVD. Below −25 ft NGVD, the groundwater temperature generally remains in the range of 75°F – 77°F (24°C – 25°C). The seasonal temperature fluctuations above −25 ft NGVD have been attributed to the heating and cooling of water in the L-31E Canal in response to seasonal changes in atmospheric conditions. Notably there is some temperature stratification in the L-31E Canal, in part due to the canal depth and limited flow. The near-surface water temperatures in the L-31E Canal are almost always warmer than the bottom temperatures, and the surface temperatures exhibit more daily variability in response to air temperature changes. Aside from the groundwater adjacent to the L-31E

Canal, it has also been reported (Ecology and Environment, Inc., 2014) that since groundwater in monitoring wells TPGW-2M and TPGW-2D is warmer than other nearby surface waters such as Biscayne Bay or fresh groundwater, the CCS might be influencing the groundwater temperatures in those wells. Based on the aforementioned evidence, it can be concluded that the environmental effects of elevated groundwater temperatures due to the operation of the CCS are inconsequential.

2.2 Heat-Balance Model of CCS

To fully understand the temperature dynamics in the CCS, it is necessary to have a validated heat-balance model of the CCS. In reviewing the documentation made available for this investigation, all indications were that such a model does not currently exist, at least not in the public domain. Historical documentation shows that a heat-balance model was developed in the early stages of operating the CCS, as reported by Ray L. Lyerly Associates (1973), however, utilization of this model has not been subsequently reported. As described by Lyerly (1973), the heat-balance model that was developed previously took into account such key components as the heat entering the water from the power-generating units, the net heat entering the water from shortwave solar radiation and longwave atmospheric radiation, and the latent heat transfer associated with evaporation. The input variables in the thermal model were the air temperature, relative humidity, wind velocity, and the net amount of radiation; the output variable was the water temperature in the CCS.

2.2.1 Heat-Balance Model Formulation

To investigate and understand the thermal dynamics within the CCS, a preliminary heat-balance model of the CCS was developed for this study. The CCS was divided into four zones as shown in Figure 3, where water in the CCS flows sequentially through zones 1, 2, 3, and 4. The four delineated zones are the same

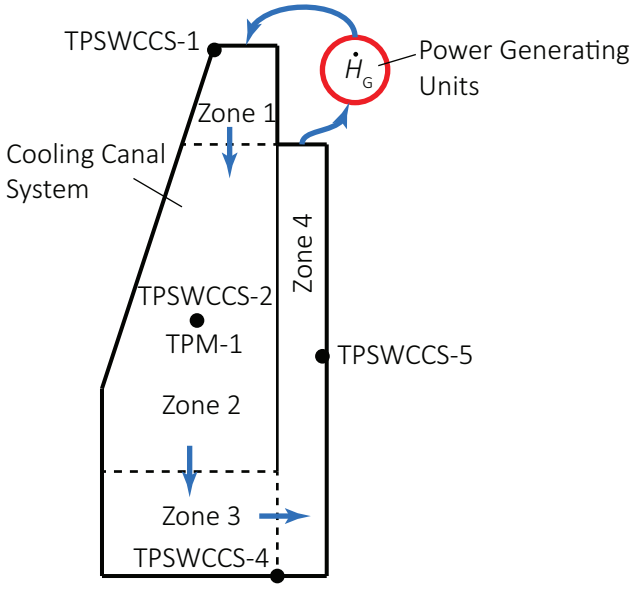

Figure 3: Cooling-canal system

zones that are used in salinity-balance model of the CCS developed by the engineering consultant for FPL.

The measurement stations that characterize conditions within each of the four CCS zones were taken as TPSWCCS-1, TPSWCCS-2, TPSWCCS-4, and TPSWCCS-5, respectively, and the approximate locations of these measurement stations are shown in Figure 3. The average-daily temperature measurements within each of the CCS zones in the period 9/1/10 – 12/7/14 are shown in Figure 4. It is apparent from these

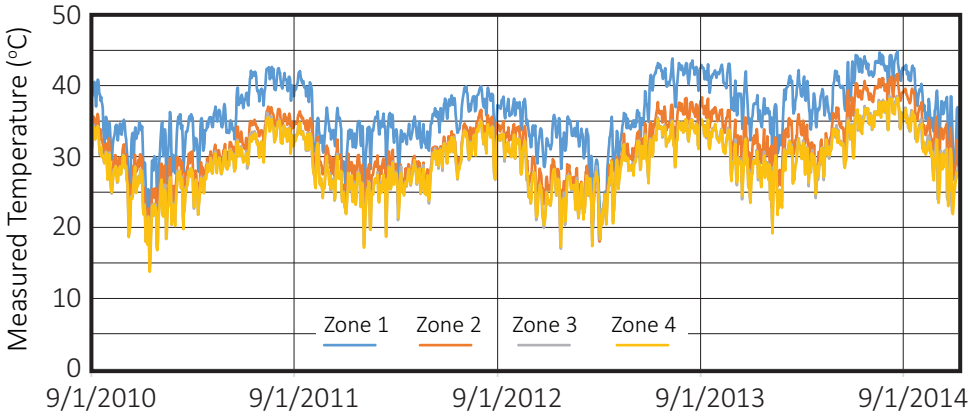

Figure 4: Temperature measurements in CCS

measurements that the temperatures in the CCS decrease noticeably from zones 1 to 3 (i.e., moving from north to south in the CCS), with much less temperature change as the water moves back to the northern (cooling-water intake) end of the CCS through zone 4. Therefore, almost all of the cooling in the CCS occurs in the south-flowing canals in the western portion of the CCS. It is further apparent from the temperature measurements shown in Figure 4 that the midsummer temperatures in 2014 (between July and August) were higher than the midsummer temperatures in previous years. For the period of record (9/1/10 – 12/7/14), the maximum measured daily-average temperature in Zone 1 was 113°F (44.9°C) recorded on 8/21/14, and the maximum measured daily-average temperature in Zone 4 was 101°F (38.3°C) recorded on 8/22/14. Since the maximum allowable temperature at the cooling-water intake is 104°F and measured temperatures in Zone 4 have been close to this limiting value (e.g., 101°F recorded on 8/22/14), there is cause for concern. Temperatures in Zone 4 near the 104°F limit could force curtailment of power generation by one or more of the power-generating units, and cause power outages in South Florida. Given the elevated temperatures that have been recorded in the CCS, is necessary to identify the fundamental reasons for these occurrences, and to determine whether such occurrences are expected to continue in the future without any changes in the CCS and/or power-plant operations. To fully understand the temperature dynamics in the CCS it was necessary to develop a heat[‡]-balance model of the CCS, which is described in the following section.

2.2.2 Heat-Flux Components

The heat fluxes within each of the CCS zones are illustrated in Figure 5, where the volumetric inflow rate and temperature are Q_1 and T_1, respectively, and the corresponding quantities on the outflow side are Q_2 and T_2. Within each zone, there are several sources of energy that are represented in Figure 5. These energy sources

[‡]In this report “heat” and “thermal energy” are used interchangeably.

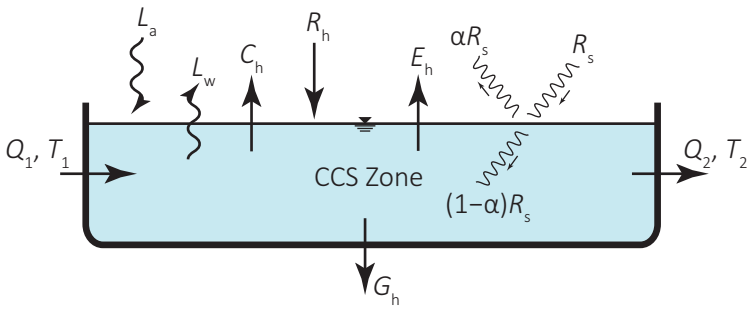

Figure 5: Energy fluxes in CCS zone

and their quantification are described below, where, for consistency with thermodynamic convention, energy added to CCS is taken as positive and energy losses are taken as negative.

Absorbed solar radiation, $(1-\alpha)R_s$. The incident solar (short-wave) radiation is represented by R_s [$EL^{-2}T^{-1}$][§], and the albedo (i.e., reflectivity) of the water surface is represented by α [dimensionless]; therefore the amount of solar radiation that is absorbed within the zone is $(1-\alpha)R_s$. The average solar radiation, R_s, for each day in the four-year study (9/1/10 – 12/7/14) was obtained from the Florida Automated Water Network (FAWN) station located on the premises of the University of Florida Tropical Research and Education Center (TREC) in Homestead, Florida. The albedo, α, of a water surface is typically on the order of 0.1 for latitudes in the range of 20° – 30° (Cogley, 1979), and a value of 0.1 was used as a reference value for this investigation. Factors such as the concentration of algae in the CCS can affect the value of α, and therefore the sensitivity of the temperature dynamics within the zone to elevated algae concentrations was investigated by varying α. The minimum value of α is equal to zero, in which case all of the incident solar radiation is absorbed by the CCS and none is reflected. Hence, α was varied within the range of 0 – 0.1.

Evaporation heat flux, E_h. Evaporation extracts heat from the CCS due to the latent heat of evaporation required to transform water from the liquid phase to the vapor phase. The evaporation heat flux, E_h [$EL^{-2}T^{-1}$], is given by

$$E_h = -E\rho_f L_v \tag{1}$$

where E [LT^{-1}] is the evaporation rate, ρ_f [ML^{-3}] is the density of fresh water, and L_v [EM^{-1}] is the latent heat of vaporization of water. The evaporation rate of water has long been known to decrease with increasing salinity (e.g., Harbeck, 1955; Salhorta et al., 1985). In the present study, daily evaporation rates, E, were calculated based on typical salinities in the CCS, measurements of water temperature, T_s [Θ], at the monitoring station within the zone, onsite measurements of air temperature, T_a [Θ] and relative humidity, RH [dimensionless] at station TPM-1, and measurements of wind speed, V_w, at station TD. The freshwater density, ρ_f, in Equation 1, was taken as 994 kg/m^3, which is the approximate density of fresh water at 35°C (95°F). The latent heat of vaporization, L_v, in Equation 1, is known to depend on both the temperature and salinity of the source (liquid) water. At a temperature of 35°C, values of L_v at salinities of 60‰ and 80‰ are 2.279 MJ/kg and 2.229 MJ/kg, respectively (Sharqawy et al., 2010), and an average of 2.254 MJ/kg was used for L_v in the energy analysis. The empirical formula used for estimating E [cm/d], from onsite meteorological

[§]Terms in square brackets indicate dimensions: E = energy, L = length, M = mass, T = time, and Θ = temperature.

measurements is

$$E = -\underbrace{C_{\mathrm{w}}(0.299 + 0.11V_{\mathrm{w}})}_{=f(V_{\mathrm{w}})}[\beta e_{\mathrm{s}}(T_{\mathrm{s}}) - \mathrm{RH}\, e_{\mathrm{s}}(T_{\mathrm{a}})] \quad (2)$$

where C_{w} [dimensionless] is a calibration constant, $f(V_{\mathrm{w}}) = C_{\mathrm{w}}(0.299 + 0.11V_{\mathrm{w}})$ is a wind function that accounts for the effect of wind on evaporation, V_{w} is the wind speed in m/s, β [dimensionless] is a factor that accounts for the effect of salinity on the saturation vapor pressure of water, and $e_{\mathrm{s}}(T)$ [kPa] is the saturation vapor pressure of water at temperature T. Equation 2 was used to calculate the evaporation for the sake of consistency with the previously developed salinity model of the CCS, where the constants C_{w} and β were taken as 0.69 and 0.885, respectively. In the salinity model, the value of C_{w} was determined by calibration, and the value of β was obtained from previous research on evaporation from saline water bodies reported by Salhorta et al. (1985). The evaporation formula given by Equation 2 has an uncertain functional form, particularly for the wind function $f(V_{\mathrm{w}})$.

Uncertainty in the wind function. Wind functions used to estimate evaporation typically have the form $f(V_{\mathrm{w}}) = a + bV_{\mathrm{w}}$, where a and b are constants. Such a wind function is used in Equation 2. In artificially heated waters, vertical convection is particulary important under low-wind conditions making specification of the value of a a key parameter. The wind function used in Equation 2 was originally proposed by Williams and Tomasko (2009) for heated waters, however, alternate formulations have been proposed by others (e.g., Brady et al., 1969; Ryan and Harleman, 1973). Notably, the formulation proposed by Ryan and Harleman (1973), and subsequently supported by Adams et al. (1975), accounts for the effect of the temperature difference between the heated water and the overlying air in specifying the convection parameter a in the wind function, which is a logical relationship that is not accounted for in the other models (including the model used in this study) and could be an important consideration in accounting for convective heat transfer at low wind velocities.

Rainfall heat flux, R_{h}. Rainfall that is cooler than the water in the CCS extracts thermal energy from the CCS because thermal energy in the CCS water is used to warm the rainwater. The heat flux, R_{h} [EL^{2}T^{-1}] due to rainfall directly on the CCS can be estimated using the relation

$$R_{\mathrm{h}} = -\rho_{\mathrm{f}} c_{p\mathrm{f}}\, d_{\mathrm{r}}(T_{\mathrm{s}} - T_{\mathrm{r}})$$

where ρ_{f} [ML^{-3}] and $c_{p\mathrm{f}}$ [EM$^{-1}\Theta^{-1}$] are the density and specific heat of the (fresh) rainwater, respectively, d_{r} is the depth of rainfall, T_{s} [Θ] is the temperature of the water in the CCS, and T_{r} [Θ] is the temperature of the rainfall. There are no direct measurements of rainfall temperature at the Turkey Point site, however, it can be estimated that during a rainfall event the ambient air can be cooled by several degrees, and the temperature of raindrops approaches that of the cooled ambient air. Cooling effects of rainfall on the ambient air have been reported to be as high as 10°C (Byers, 1949). On a global average, raindrops can have temperatures in the range of 32°F – 80°F (0°C – 27°C). For purposes of the present analysis, the temperature of the rainfall, T_{r}, was assumed to be 68°F (20°C), and the corresponding values of ρ_{f} and $c_{p\mathrm{f}}$ were taken as 998 kg/m^3 and 4.180 kJ/kg·°C, respectively. The temperature dynamics in the CCS zones are relatively insensitive to the assumed temperature of the rainfall.

Atmospheric longwave radiation, L_{a}. Any body of matter whose temperature is above absolute zero emits longwave radiation. Longwave radiation, L_{a} [W/m^2] emitted by the atmosphere can be estimated us-

ing the relation (Chin, 2013)

$$L_{\mathrm{a}} = \sigma(T_{\mathrm{a}} + 273)^4(0.6 + 0.031\sqrt{\mathrm{RH}\, e_{\mathrm{s}}(T_{\mathrm{a}})}(1 - R_{\mathrm{L}})$$

where σ is the Stefan-Boltzmann constant ($= 4.903 \times 10^{-9}$ MJ·m^{2}K^{-4}d^{-1}), T_{a} [°C] is the air temperature, RH [dimensionless] is the relative humidity, $e_{\mathrm{s}}(T_{\mathrm{a}})$ [mm Hg] is the saturation vapor pressure of water at temperature T_{a}, and R_{L} is the longwave reflection coefficient that can be taken as 0.03. On cloudy days, atmospheric longwave radiation can be the greatest source of thermal energy at the water surface.

Water longwave radiation, L_{w}. Water in the CCS also emits longwave radiation by virtue of its temperature being greater than absolute zero. Longwave radiation, L_{w} [W/m^2] emitted by the water in the CCS can be estimated using the relation (Chin, 2013)

$$L_{\mathrm{w}} = -\epsilon\sigma(T_{\mathrm{s}} + 273)^4$$

where ϵ is the emissivity of water that can be estimated as 0.97 [dimensionless], σ is the Stefan-Boltzmann constant as given previously, and T_{s} [°C] is the temperature of the water in the CCS.

Heat interchange with surrounding aquifer, G_{h}. The CCS exchanges heat with the surrounding aquifer via seepage of groundwater into and out of the CCS, and conduction of heat between water in the CCS and groundwater in the surrounding aquifer. It is to be expected that the region immediately surrounding the CCS is normally cooler than the water in the CCS, in which case there will be cooling of the CCS water due to heat conduction between the CCS and the surrounding aquifer, cooling due to seepage inflow from the surrounding aquifer into the CCS, and no cooling or heating due to seepage outflow from the CCS into the surrounding aquifer. The cooling heat flux due to conduction can be assumed to negligible compared to the heat flux due to seepage inflow. The heat flux G_{h} [EL^{-2}T^{-1}] due to seepage inflow is proportional to the temperature difference between the water in the CCS and the groundwater in the surrounding aquifer and can be estimated by the relation

$$G_{\mathrm{h}} = -\rho_{\mathrm{g}} c_{p\mathrm{g}} \frac{Q_{\mathrm{sg}}}{A_{\mathrm{s}}} \Delta T_{\mathrm{sg}}$$

where ρ_{g} [ML^{-3}] and $c_{p\mathrm{g}}$ [EM$^{-1}\Theta^{-1}$] are the density and specific heat, respectively, of the groundwater surrounding the CCS, Q_{sg} [L^{3}T^{-1}] is the seepage inflow to the CCS from the surrounding aquifer, A_{s} [L^2] is the area of the CCS zone, and ΔT_{sg} [Θ] is the difference between the temperature in the CCS, T_{s} [Θ], and the temperature on the surrounding groundwater, T_{g} [Θ] (i.e., $\Delta T_{\mathrm{sg}} = T_{\mathrm{s}} - T_{\mathrm{g}}$)

Conduction heat flux, C_{h}. The conduction heat flux is associated with the sensible transfer of heat between the CCS water and the air above the CCS. The conduction heat flux, C_{h} [W/m^2] can be estimated using the empirical relation (Chin, 2013; Chapra, 1997)

$$C_{\mathrm{h}} = -c_{\mathrm{B}} f(V_{\mathrm{w}})\,(T_{\mathrm{s}} - T_{\mathrm{a}})$$

where c_{B} is Bowen's coefficient, and $f(V_{\mathrm{w}})$ is the wind function as defined in Equation 2. Following the guidance given in Chin (2013) and Chapra (1997), the value of c_{B} can be estimated as 0.063. According to Martin and McCutcheon (1998), sensible heat transfer from lakes and reservoirs to the overlying air due to conduction and convection is a relatively small component of the heat balance

equation that is poorly understood, and Brown and Barnwell (1987) have noted that the conduction heat flux from lakes and reservoirs to the overlying air calculated by heat-transfer theory is normally small enough to neglect. Given the aforementioned considerations, conduction of heat between the CCS and the overlying air was neglected in this analysis.

Based on the component heat fluxes described above, the net heat flux, $\dot{H}_{\mathrm{C}}$ [$\mathrm{EL^{-2}T^{-1}}$], into the CCS is given by

$$\dot{H}_{\mathrm{C}} = \sum_{i=1}^{4} \left\{ \left[(1-\alpha) R_{\mathrm{s}} + E_{\mathrm{h}} + R_{\mathrm{h}} + L_{\mathrm{a}} + L_{\mathrm{w}} + G_{\mathrm{h}} \right]_i A_i \right\} \tag{3}$$

where i is an index that refers to each zone within the CCS, A_i [$\mathrm{L^2}$] is the area of Zone i, and the summation is over the four zones within the CCS. The areas of each of the zones in the CCS are given in Table 1, and the total area of the CCS is approximately 1907 ha (= 4712 ac). The heat extracted from the CCS by pumping

Table 1: CCS Zonal Areas in Energy and Salinity Models

Zone	**Area** (ha)
1	368.0
2	795.1
3	396.6
4	347.0
Total	1906.7

cooler water from the ID into the CCS was calculated in a similar manner to the method used to calculate the cooling effect of rainfall, where the "effective" rainfall rate is equal to the volume of water pumped from the ID divided by the area of the CCS. Assuming (conservatively) that the temperature difference between the ID water and the CCS water is 10°C (50°F), the cooling effect of pumped ID water was found to be negligible compared with other component fluxes in the heat-balance equation.

2.2.3 Heat-Balance Equations

Under steady-state conditions, conservation of thermal energy requires that the net rate at which heat is added to the CCS is equal to the difference in thermal energy between the water leaving the CCS and the water entering the CCS. This relationship is expressed by the following equation,

$$\dot{H}_{\mathrm{C}} = \rho_{\mathrm{s}} c_{p\mathrm{s}} Q (T_4 - T_1) \tag{4}$$

where ρ_{s} and $c_{p\mathrm{s}}$ are the density and specific heat of the CCS water, Q is the flow rate of water through the CCS, T_4 the temperature of the cooling water at the intake of the power plant (in Zone 4), and T_1 is the temperature of the cooling water at the discharge from the power plant (in Zone 1). If the power-generating units add heat to the water at a rate $\dot{H}_{\mathrm{G}}$, then between the intake and discharge end of the power-generating units the heat-balance equation is given by

$$\dot{H}_{\mathrm{G}} = \rho_{\mathrm{s}} c_{p\mathrm{s}} Q (T_1 - T_4) \tag{5}$$

Combining Equations 3, 4, and 5 requires that the heat rejection rate in the power-generating units, $\dot{H}_{\mathrm{G}}$, is related to the net rate at which heat is added to the CCS, $\dot{H}_{\mathrm{C}}$, by the relation

$$\dot{H}_{\mathrm{G}} = -\sum_{i=1}^{4} \left\{ \left[(1-\alpha) R_{\mathrm{s}} + E_{\mathrm{h}} + R_{\mathrm{h}} + L_{\mathrm{a}} + L_{\mathrm{w}} + G_{\mathrm{h}} \right]_i A_i \right\} \tag{6}$$

This equation can be used to estimate the heat-rejection rate, $\dot{H}_{\mathrm{G}}$, of the power-generating units based on field measurements that are used to calculate the terms on the righthand side of Equation 6. In cases where daily time steps are used, estimated values of $\dot{H}_{\mathrm{G}}$ might fluctuate about a mean value and be difficult to discern. In such cases, the average heat-rejection rate, $\langle \dot{H}_{\mathrm{G}} \rangle_J$, over a period of J time steps can be estimated using the relation

$$\langle \dot{H}_{\mathrm{G}} \rangle_J = \frac{1}{J\Delta t} \sum_{j=1}^{J} \dot{H}_{\mathrm{G}} \Delta t \tag{7}$$

where Δt is the duration of each time step. In accordance with Equation 7, a constant heat rejection rate can be recognized by plotting the cumulative estimated heat rejection rate, $\sum_{j=1}^{J} \dot{H}_{\mathrm{G}} \Delta t$, versus time, $J\Delta t$, which would would result in a straight line of constant slope equal to $\langle \dot{H}_{\mathrm{G}} \rangle_J$. This relationship was used in this study to identify periods of constant heat rejection rate of the power-generating units that utilize the CCS.

2.2.4 Model Results

The heat-balance model was applied to each of the four zones within the CCS to determine the net heat flux into each zone, and the results from all zones were combined to determine the net heat flux into the entire CCS. The energy model was applied at daily time steps for the period of record 9/1/10 – 12/7/14. The thermal-energy dynamics within each of the CCS zones are similar, and the fluctuations of the heat-flux components in Zone 1 will be used to demonstrate the thermal-energy dynamics within each zone.

Zone 1 heat-flux components. The longwave radiation and shortwave solar energy fluxes as a function of time are shown in Figure 6(a), and the evaporation and rainfall heat fluxes as a function of time are shown in Figure 6(b). It is apparent that the shortwave and longwave energy fluxes vary seasonally, and that there

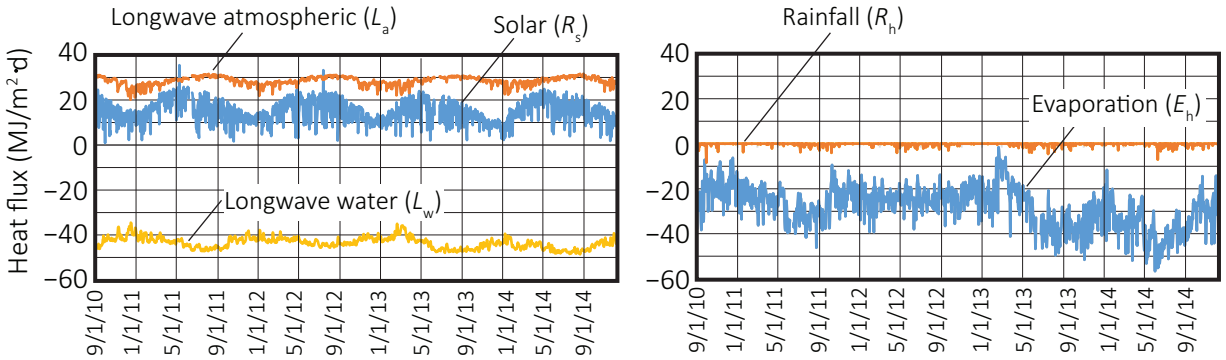

(a) Longwave and solar energy (b) Rainfall and evaporation energy

Figure 6: Energy fluxes in Zone 1

is much more seasonal variation in the shortwave solar radiation than in the longwave radiation. The net longwave radiation has a cooling effect (i.e. net negative heat flux) which contributes to a net-radiation cooling of the CCS water at night when the solar radiation is effectively zero. It is apparent from Figure 6(b) that evaporation and rainfall generally have a cooling effect, with evaporation usually having the greater cooling effect and rainfall having a lesser cooling effect. The convective heat flux between the CCS and the adjacent groundwater, G_{h}, is not shown in Figure 6 because the magnitude of G_{h} is generally much smaller that the heat flux due to rainfall and therefore has a minimal impact on the heat balance within the CCS.

Heat rejection rate of the power-generating units. To determine the thermal dynamics in the entire CCS, the component heat fluxes were determined for each zone within the CCS, and these heat fluxes were combined in accordance with Equation 6 to determine the thermal energy that is added to the CCS by the power plant (i.e., the heat-rejection rate). The cumulative heat-rejection from the power plant as a function of time for the entire CCS is shown in Figure 7. It is apparent from Figure 7 that there are two

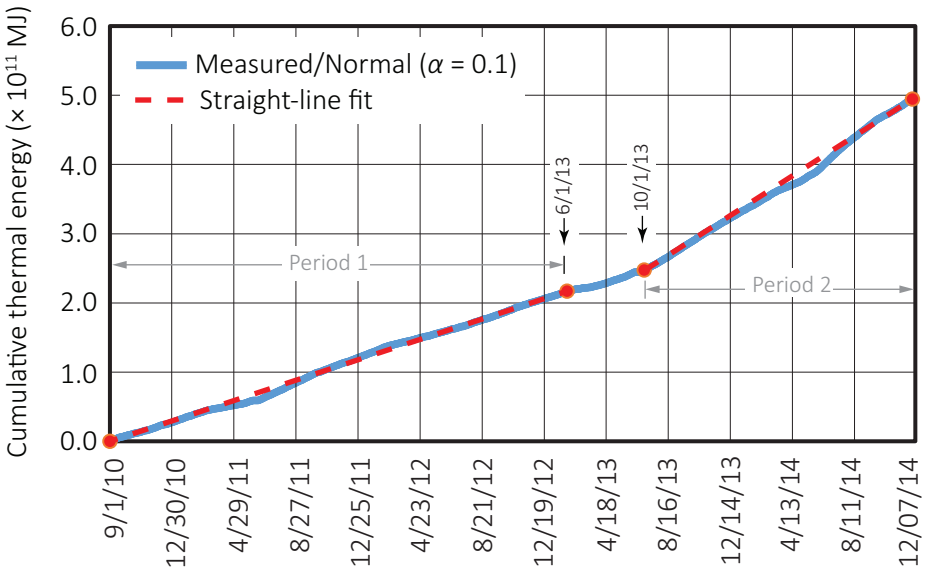

Figure 7: Cumulative heat rejection rate from the power plant

periods during which the heat rejection rate is approximately constant. The first period, shown as Period 1 in Figure 7, covers the time interval 9/1/10 – 2/1/13, and the second period (Period 2) covers the time interval 7/1/13 – 12/1/14. Notably, Period 1 includes the pre-uprate period before May 2013 and Period 2 includes the post-uprate period after May 2013. During Period 1, the average heat-rejection rate is estimated to be around 2800 MW, and during Period 2 the average heat-rejection rate is estimated to be around 5500 MW. Although these estimated heat rejection rates are preliminary estimates and derived from an uncalibrated heat-balance model, the distinct difference in heat-rejection rates between the two periods is clear, and the numerical estimates of the heat-rejection rates during these two periods are reasonable given the capacities of the power-generating units serviced by the CCS and the energy efficiencies normally associated with both fossil-fuel and nuclear power plants. A logical inference from the results shown in Figure 7 is that the uprate in power-generating capacity of the two nuclear units (Units 3 and 4) has caused the total heat-rejection rate from the power plant to increase significantly. This finding is not inconsistent with the condition that the post-uprate generating capacity of the power plant served by the CCS is less than the pre-uprate generating

capacity (due to Unit 2 operating in synchronous generator mode). This is so because in the post-uprate generating capacity there is a significant shift from fossil-fuel generation to nuclear-power generation, and nuclear-power units are known to have a much higher heat-rejection rates to cooling water than fossil-fuel generating units, which release a significant portion of their waste heat in flue-gas emissions.

Effect of algae. It is assumed that the algae content of the CCS affects the heat balance in the CCS by increasing the amount of solar energy that is absorbed by the CCS. Consequently, the effect of algae in the CCS was investigated by reducing the albedo (i.e., reflectivity), α, of the water surface from 0.1 to 0.0 starting on January 1, 2014. An albedo of 0.1 was used in the "normal" simulations presented in Figure 7 since this is the typical value of α that is associated with water surfaces at subtropical latitudes; this corresponds to 90% of the incident solar radiation being absorbed by the water in the CCS. Assuming that the effect of algae is to retain more solar heat, then taking $\alpha = 0$ reflects the extreme case where the CCS with high concentrations of algae absorbs 100% of the incoming solar radiation. The effect of reducing α from 0.1 to 0.0 on the estimated cumulative heat-rejection rate is shown in Figure 8. It is apparent that the

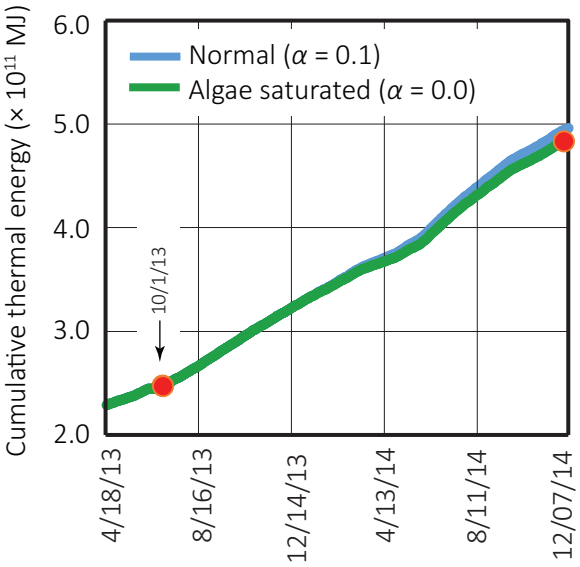

Figure 8: Estimated algae effect on estimated cumulative heat rejection rate from the power plant

impact of the higher absorption rate of solar energy attributed to high algae concentrations is relatively small compared with the heat rejection rate of the power-generating units. In quantitative terms, the increased rate of heating of the CCS due to reduced reflection of solar energy is around 400 MW, compared with a normal heat rejection rate of around 5700 MW (in 2014). This indicates that the (maximum) rate of increased heating caused by algae is only around 7% of the normal heat-rejection rate, and hence there is a relatively small heating effect caused by algae in the CCS.

Relationship between increased net heat flux and temperature. An increased heat-rejection rate would be expected to increase the temperature in the CCS relative to the temperature of the overlying air. Representing the temperature in the CCS as T_{s}, and the temperature of the overlying air as T_{a}, this temperature difference is $T_{\mathrm{s}} - T_{\mathrm{a}}$. The variation of $T_{\mathrm{s}} - T_{\mathrm{a}}$ as function of time for each of the four CCS zones is shown

in Figure 9, where the average temperature difference during Period 1 and Period 2 are shown as horizontal lines. It is apparent from Figure 9 that the increase in the average heat-rejection rate from Period 1 to

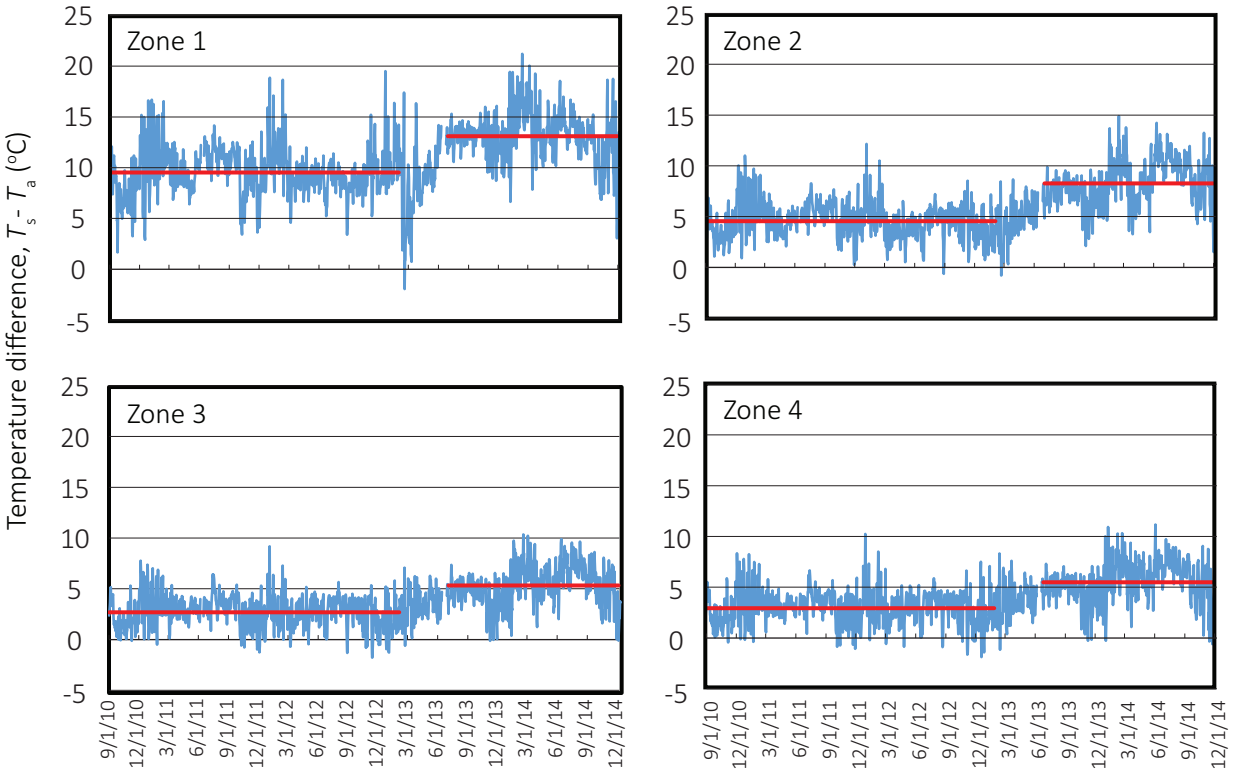

Figure 9: Temperature differences between CCS and overlying air. Horizontal lines show intervals of constant heat-addition rates.

Period 2 corresponds to an increase in the average value of $T_\mathrm{s} - T_\mathrm{a}$. Representing the average value of $T_\mathrm{s} - T_\mathrm{a}$ during Period 1 as $\overline{\Delta T}_1$ and the average value of $T_\mathrm{s} - T_\mathrm{a}$ during Period 2 as $\overline{\Delta T}_2$, these averaged values for each CCS zone are shown in Table 2, along with the corresponding standard deviations, S_1 and S_2, respectively. These results show that in Zone 1, which accepts the cooling-water discharge, the average temperature difference between the CCS and the overlying air has increased from 9.6°C (18°F) to 13.1°C (23.6°F), which corresponds to an average temperature increase of 3.5°C (6.3°F). In Zone 4, which contains the cooling-water intake, the average temperature difference between the CCS and the overlying air has increased from 2.8°C (5.0°F) to 5.4°C (9.7°F), which corresponds to an average temperature increase of 2.6°C (4.7°F). These changes in average temperature can be contrasted with previous (pre-uprate) predictions made by FPL's engineering consultants in 2008 where it was anticipated that the uprate of Units 3 and 4 would cause a maximum temperature increase of 1.4°C (2.5°F) in the discharged cooling water (to Zone 1) and an increase of 0.5°C (0.9°F) in the temperature of the intake water (from Zone 4). The standard deviations of the temperature fluctuations are similar across all zones, and have shown relatively modest decreases between the pre-uprate and post-uprate periods. Of particular interest, in Zone 1 the standard deviation decreased from 3.8°C (6.8°F) to 3.3°C (5.9°F), and in Zone 4 the standard deviation decreased from 3.9°C (7.0°F) to 3.5°C (6.3°F).

Table 2: Temperature Statistics in CCS

	Period 1		**Period 2**			
	$\overline{\Delta T}_1$	S_1	$\overline{\Delta T}_2$	S_2	$\overline{\boldsymbol{\Delta T}}_{\mathbf{2}} - \overline{\boldsymbol{\Delta T}}_{\mathbf{1}}$	
Zone	(°C)	(°C)	(°C)	(°C)	(°C)	(°F)
1	9.6	3.8	13.1	3.3	3.5	6.3
2	4.6	3.7	8.4	3.7	3.8	6.8
3	2.9	3.9	5.5	3.6	2.6	4.7
4	2.8	3.9	5.4	3.5	2.6	4.7

Thermal efficiency. The thermal efficiency, η_{t}, of the CCS is a measure of the ability of the CCS to cool the water down to the background air temperature. The thermal efficiency of the CCS was previously measured by Lyerly (1998) using the relation

$$\eta_{\mathrm{t}} = 1 - \frac{T_{\mathrm{i}} - T_{\mathrm{a}}}{T_{\mathrm{d}} - T_{\mathrm{a}}} \tag{8}$$

where T_{d} and T_{i} are the temperatures of the cooling water at the discharge and intake ends of the power plant, respectively, and T_{a} is the temperature of the ambient air above the CCS. The thermal efficiency of the CCS can be estimated using Equation 8 by replacing $T_{\mathrm{d}} - T_{\mathrm{a}}$ by the average value of $T_{\mathrm{s}} - T_{\mathrm{a}}$ in Zone 1, and replacing $T_{\mathrm{i}} - T_{\mathrm{a}}$ by the average value of $T_{\mathrm{s}} - T_{\mathrm{a}}$ in Zone 4. Using the averaged temperature differences given in Table 2 in Equation 8 gives:

$$\text{Period 1: } \eta_{\mathrm{t}} = 1 - \frac{2.8}{9.6} = 0.71, \qquad \text{Period 2: } \eta_{\mathrm{t}} = 1 - \frac{5.4}{13.1} = 0.59$$

These results indicate that the thermal efficiency of the CCS in Period 1 is around 70% and the thermal efficiency of the CCS in Period 2 is around 60%. Hence, the thermal efficiency of the CCS has apparently decreased between Period 1 and Period 2. The reason for this decrease in thermal efficiency is not readily apparent and could be due to a variety of factors, including increased thermal loading and increase algae concentrations in the CCS. It should be noted that the thermal efficiency of 86% reported by Lyerly (1998) is not directly comparable to the values calculated here, since the additional cooling between the discharge location and the Zone 1 temperature measurement station, as well as the additional cooling between the intake location and the Zone 4 temperature measurement location are not taken into account in the present analysis.

2.2.5 Conclusions

The results derived from the heat-balance model indicate that the rate of heat addition to the CCS has increased significantly during the period of record, and that the increased heat-addition rate is manifested in an increase in the average temperature in the CCS relative to the temperature of the overlying air. It appears that the most likely cause for the increased heat-addition rate is an increased heat-rejection rate from the power-generating units. Notably, the increased heat-addition rate began shortly after the beginning of the post-uprate period. As a result of the increased heat addition to the CCS, the average temperature in the intake zone (Zone 4) has increased by approximately 2.6°C (4.7°F). Interestingly, this measured increase in

average temperature is slightly greater than the increase in the maximum allowable operating temperature at the intake location of 2.2°C (4.0°F)[¶] approved by the Nuclear Regulatory Commission in 2014. Therefore, the increased maximum allowable operating temperature has not reduced the probability of the intake temperatures exceeding the threshold value, and might have slightly increased the probability of exceeding the threshold temperature. This serves as a cautionary note regarding further increases in power generation beyond 2014 levels without providing a supplementary system to cool the water in the CCS. Others have cited increased algae concentrations in the CCS as being as a possible reason for elevated temperatures of the water in the CCS. However, a sensitivity analysis indicates that changes in the algae-influenced solar reflectivity of the CCS within a realistic range are unlikely to have been of sufficient magnitude to cause the observed changes in temperature, nor stimulate the sudden change in heat-addition rate that was observed almost immediately after the beginning of the post-uprate period. There are indications that the thermal efficiency of the CCS has decreased significantly between the pre-uprate and post-uprate periods. Further investigation is recommended to confirm this finding and to identify the factor(s) causing the reduced thermal efficiency.

Limitations of the heat-balance model. The heat-balance model developed for this study is based on the best estimates of all of the heat-balance components that influence the temperature in the CCS. However, the heat-balance model has not been calibrated due to lack of available data for calibration. Data required to calibrate the heat-balance model would include synoptic measurements of the flow rate and temperature differences between the intake and discharge structures of the power-generating units, and synoptic temperatures and flow rates at the inflow and outflow faces of each CCS zone. Calibration of the heat-balance model would not necessarily change the key inferences that have been drawn from the uncalibrated model, namely that there has been a significant increase in the heat-rejection rate from the power-generating units during the post-uprate period, and that increased algae concentrations and increased ambient temperatures are not the most likely causes of elevated temperatures in the CCS. Further development of a calibrated heat-balance model is warranted to confirm the conclusions that have been drawn.

3 Salinity Variations in the Cooling Canals

Salinity is defined as the mass of dissolved salts per unit mass of solution, and is usually reported directly in units of either parts per thousand (‰) or as a dimensionless number on the practical salinity scale 1978 (PSS-78). Salinities are sometimes expressed indirectly in terms of chlorinity (mg/L chloride) or conductance (mS/cm). In this report, salinities are expressed in units of parts per thousand (‰), which gives salinities approximately equal in magnitude to salinities expressed in PSS-78. As reference points, average seawater at 25°C has a salinity of 35‰, a chlorinity of 19.84 g/L, and a specific conductance of 54.7 mS/cm. Hypersaline water is typically defined as water with a salinity greater than 40‰ or a specific conductance greater than 61.5 mS/cm, and brine is typically defined as water with a salinity greater than 50‰. These hypersalinity and brine thresholds are routinely exceeded in the CCS, and therefore water within the CCS can be properly classified either as being hypersaline or as brine.

[¶]From 37.8°C to 40°C (100°F to 104°F)

3.1 Results from Previous Studies

There has been a continuous upward trend in salinity since the CCS began operation in August 1973, and this trend is clearly apparent in Figure 10, which shows the maximum reported salinities in the CCS since the initial NPDES report was submitted in 1973. The long-term trend of increasing salinity shown in Figure 10

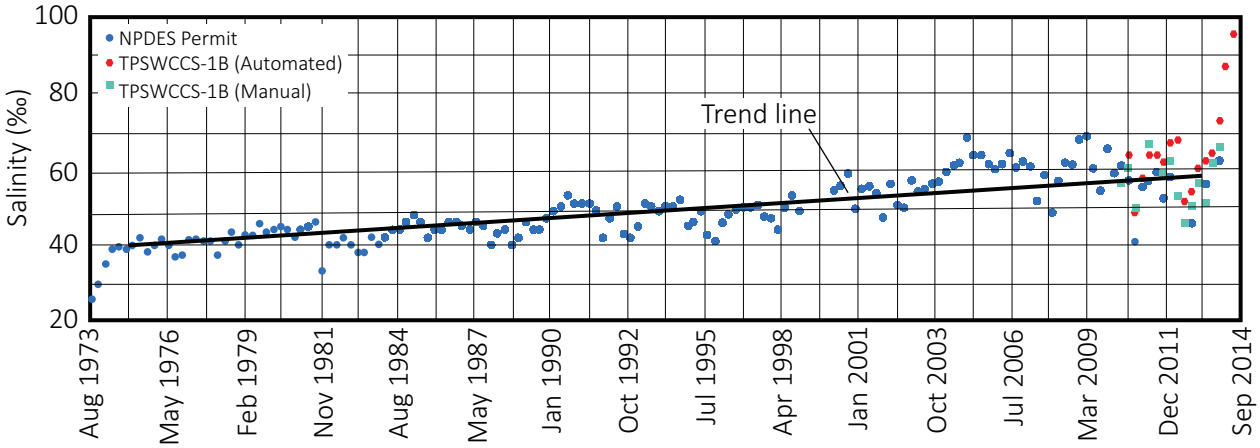

Figure 10: Maximum observed salinities in the CCS since initial operation

can be approximated as being linear (as shown by the linear trend line) with a salinity increase of around 5‰ per 10 years. It is also apparent from Figure 10 that the rate of increase in salinity might have accelerated since 2013. The salinity in the CCS when it was first put into operation was around 26.5‰, with the contemporaneous salinity in Biscayne Bay being around 33‰ (Lyerly, 1973). The average CCS salinity in 1998 was reported to be in the range of 38 – 50‰ (Lyerly, 1998), and in May 2014, the salinity in the CCS was reported to be as high as 95‰.

Salinity-control processes. The key processes affecting the salinity in the CCS are: rainfall, evaporation, and groundwater exchange between the CCS and the surrounding aquifer. Average annual rainfall at Turkey Point is approximately 60 inches, and the natural annual evaporation at Turkey Point is approximately equal to the average annual rainfall. Actual evaporation of water from the CCS exceeds natural evaporation due to the elevated temperatures in the CCS. The steady increase in salinity since operation of cooling canals began in the early 1970s (as shown in Figure 10) has been most commonly attributed to evaporation excess over rainfall.

3.1.1 Historical Chloride Levels

Chloride concentrations (i.e., chlorinities) in the CCS between June 2010 and June 2012 were in the range of 26 – 46 g/L with an average chlorinity of 33.9 g/L. The average chlorinity in Biscayne Bay during the same period was 18.9 g/L (Ecology and Environment, Inc., 2012). There is little difference (less than 10%) in chloride concentration between samples collected near the surface or near the bottom at any given sampling location within the CCS canals. Chloride concentrations in the CCS during the post-uprate period were observed in range of 27.0 – 49.8 g/L, with the highest values observed in March 2014 and the lowest values in June 2013 (Ecology and Environment, Inc., 2014).

3.1.2 Historical Specific Conductance Levels

Specific conductances in the CCS between June 2010 and June 2012 were in the range of 70 – 90 mS/cm. Specific conductance in the CCS has been rising since the beginning of the dry season in 2014 and reached over 120 mS/cm in May 2014. The average post-uprate specific conductance for all CCS stations was reported as 92.6 mS/cm, and this average value was over 15 mS/cm higher than the average value reported in the pre-uprate period.

3.2 Salinity-Balance Model of CCS

The salinity-balance model of the CCS that is currently being used to simulate salinity variations in the CCS was developed by engineering consultants for FPL. The salinity-balance model uses a finite-control-volume approach in which the control volume is defined to include the canals of the CCS and the adjacent interceptor ditch (ID). The salinity-balance model is closely related to a companion water-balance model, with both models having been developed by the same contractor and described by Ecology and Environment, Inc. (2012). For purposes of the current analyses, this previously developed model will be accepted as valid and the relevant components of the model formulation are described in the following section.

3.2.1 Salinity-Balance Model Formulation

Component salinity fluxes into and out of the defined control volume are determined by multiplying the water (volume) flux by the corresponding salinity. The components of the water balance model are the lateral and vertical seepage into the CCS, blowdown water (i.e., additional water pumped from other units to the CCS), rainfall (including runoff from earth berms between canals), and evaporation. The key features of the salinity model are as follows:

- The base of the control volume is assumed to be the bottom of the ID and the cooling canals, whose elevation ranges from approximately -3 ft feet NAVD[‖] to approximately -30 ft NAVD. The elevation of bottom of the ID is approximately -20 ft NAVD. Sloping sidewalls of the canals in the CCS are taken into account by expressing the water-surface area as a function of the water-surface elevation(s) in the CCS.

- Lateral seepage of water and salt between the L-31E Canal and the control volume is calculated directly from the product of the calibrated hydraulic conductivity and the difference in water-surface elevations between the L-31E Canal and the ID.

- Lateral seepage of water and salt between Biscayne Bay and the control volume is calculated directly from the product of the calibrated hydraulic conductivity and the difference in water-surface elevations between the CCS and Biscayne Bay.

- Vertical seepage of water and salt through the bottom of the control volume is calculated directly from the product of the calibrated hydraulic conductivity and the difference in the water-surface elevations in the CCS and the measured and estimated piezometric heads beneath the CCS.

- Evaporation is estimated using Equation 2, which uses meteorological data collected from meteorological stations in and immediately to the north and south of the CCS.

[‖] "NAVD" refers to the NAVD 88 datum.

- Rainfall is estimated using Next Generation Weather Radar (NEXRAD) precipitation data provided by the SFWMD. Runoff into the control volume from earth berms between canals is used as a calibration parameter and is initially assumed to be 50% of the rainfall that falls on the berms.
- Added water from Units 3 and 4 are assumed to be freshwater (non-saline); Unit 5 blowdown salinities are adjusted to between 20% and 80% of seawater (35‰), with the exact percentage used as a calibration parameter.
- The ID control system is simulated to operate primarily between the months of January and June; with pumping rates as high as 50 mgd and averaging 4.5 mgd over the calibration period.
- The water-budget model is calibrated first by minimizing the errors between the simulated and observed storage in the control volume. Parameters adjusted during calibration of the water-budget model included the hydraulic conductivities in the aquifer adjacent to and beneath the CCS, an evaporation factor that adjusts the coefficients in the wind function, the amount of runoff that enters the control volume as percentage of precipitation, and the amount of Unit 5 cooling-tower water that is lost to evaporation before entering the CCS. The salinity model uses measured salinities in and around the CCS.

Calibrated values of the horizontal hydraulic conductivities in the aquifer surrounding the control volume have been found to be in the range of 500 – 950 ft/d, and calibrated values of the vertical hydraulic conductivities beneath the control volume have been found to be in the range of 0.1 – 4 ft/d. Vertical hydraulic conductivities beneath the northern discharge canals and beneath the return canals, where it is assumed deeper canals intersect highly permeable material underlying the muck and Miami Limestone Formation, were calibrated to have (higher) vertical hydraulic conductivities of 3.8 ft/d and 4 ft/d, respectively. Lower vertical hydraulic conductivities of 0.1 ft/d were calibrated for the mid- and southern portions of the discharge canals, as well as the southern portion of the return canals. Calibration of the salinity model was done entirely by the FPL contractor.

3.2.2 Previous Model Results

The model was run to simulate salinity variations both before the uprate (i.e., before November 2012) and after the uprate (i.e., after May 2013). The results of these model simulations are useful in understanding the salinity dynamics in the CCS and are described below.

Pre-uprate model results. The salinity model was calibrated for a 22-month pre-uprate period and the results showed an average volume outflow rate from the CCS of 0.62 mgd, with monthly-averaged outflow rates ranging from -46.6 mgd (October 2010) to $+52.1$ mgd (September 2010) (Ecology and Environment, Inc., 2012). Net flow through the bottom of the CCS was generally outward between the dry-season months of September through February, and inward during the wet-season months. Average inflow from precipitation during the wet season was more than twice that for the dry season. It was reported that vertical flows into and out of the control volume were substantially larger than lateral flows.

Post-uprate model results. A second round of salinity-model results was reported for the post-uprate period of June 2013 – May 2014 (Ecology and Environment, Inc., 2014). The results showed an average outflow rate of 3.26 mgd, with monthly-averaged outflow rates ranging from -31.1 mgd (June 2013) to

$+19.6$ mgd (July 2013). During the pre-uprate and interim operating period, (September 2010 to May 2013), precipitation accounted for 39.4% of inflowing water to the CCS and evaporation accounted for 63.7% of the outflowing water from the CCS. There was an average rate of increase of salt in the CCS during the post-uprate period of 2.2×10^6 lb/d, which was attributed primarily to the combined effects of low rainfall and high evaporation. These model simulations were able to match the summer 2014 rise in salinity from approximately 60‰ to approximately 90‰.

3.2.3 Analysis of Salinity Dynamics

The primary drivers of salinity variations in the CCS are rainfall, evaporation, and seepage exchanges between the CCS and the surrounding aquifer. Pumpage from the ID can also influence salinity variations in the CCS, but its role is secondary to that of the aforementioned processes. Evaporation increases the salinity, rainfall and ID pumpage decrease the salinity, and seepage interchange with the surrounding aquifer can either increase or decrease the salinity depending on other factors.

Salinity variations under dry conditions. Under conditions of no rainfall (i.e., dry conditions), salinity in the CCS is primarily controlled by evaporation, and the salinity in the CCS steadily increases with time. Evaporation removes pure water from the CCS, and the volume of pure water that is evaporated is replenished by the seepage of saline water into the CCS from the surrounding aquifer. Since the CCS is directly connected to the surrounding aquifer, the water surface elevation within the CCS remains close to the water-table elevation in the surrounding aquifer which changes over relatively long time scales (viz. months) compared to the shorter time scales (viz. days, weeks) over which significant salinity variations are observed. Small differences between the water-surface elevations in the CCS and the water-table elevations in the adjacent aquifer are proportional to the seepage interchange between these two bodies of water. Over shorter time scales (viz. days) the evaporated volume of pure water is approximately equal to the seepage inflow volume of saline water, and the volume of water within the CCS remains approximately constant. This mechanism results in an increased mass of salt in an unchanged CCS volume, and hence an increase in salinity.

Salinity variations under wet conditions. When rainfall occurs (i.e., wet conditions), salinity is primarily controlled by the difference between evaporation and rainfall. Conditions under which evaporation exceeds rainfall result in the net removal of pure water from the CCS and the dynamics of salinity variations under this condition are similar to those described previously for evaporation without rainfall. Hence, for time intervals where evaporation exceeds rainfall, the salinity in the CCS can be expected to increase. For time intervals where rainfall exceeds evaporation, there is a net inflow of (approximately) pure water into CCS that is equal to the difference between the rainfall and evaporation volumes, and this inflow is approximately balanced by the volume of saline water that seeps out of the CCS into the surrounding aquifer. The salinity of the seepage outflow is approximately equal to the salinity of the water within the CCS. This mechanism results in a decreased mass of salt in the CCS in an unchanged volume, and hence a decrease in salinity.

Salinity variations under ID pumping. Pumping water from the ID into the CCS has a relatively minor effect on the salinity in the CCS relative to rainfall and evaporation, since the volume of pumped water is relatively smaller and the difference in salinity between the pumped water and the water in the CCS is also less than for evaporation and rainfall.

3.2.4 Demonstration of Salinity Dynamics

The mechanism driving salinity changes in the CCS can be demonstrated using the previously calibrated salinity model. The cumulative rainfall, evaporation, seepage inflow, ID pumpage, and water storage (= net inflow) within the CCS between September 2010 and April 2014 are shown in Figure 11. It is apparent

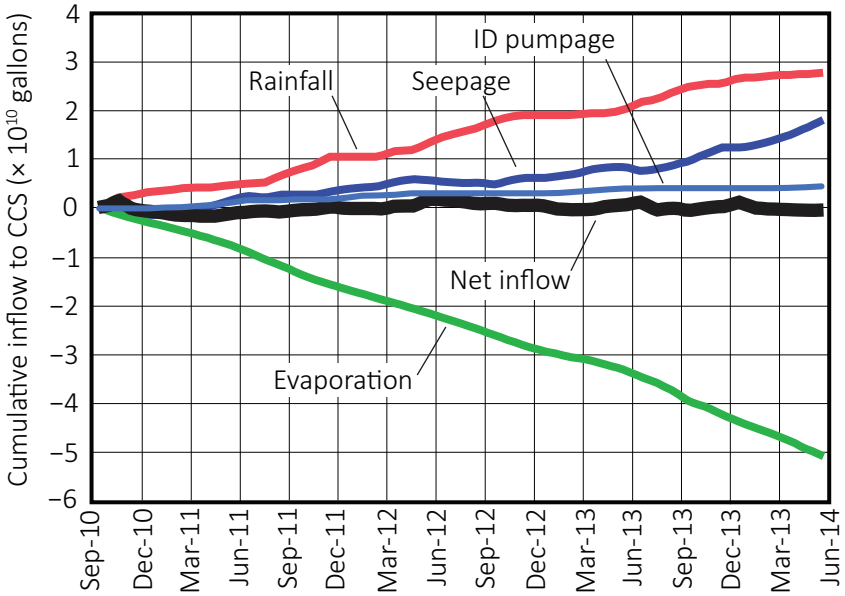

Figure 11: Water inflow into CCS

from Figure 11 that the storage in the CCS remains relatively constant compared with cumulative rainfall, evaporation, ID pumpage, and seepage inflow. Further, it can be asserted from Figure 11 that the seepage inflow adjusts to the difference between evaporation and rainfall-plus-ID-pumpage so as to keep the volume of water within the CCS approximately constant. The cumulative evaporation and rainfall in Figure 11 show approximately linear trends, with the evaporation trend line showing an average evaporation rate of approximately 39 mgd, and the rainfall trend line showing an average rainfall rate of approximately 21 mgd.

Distribution of seepage inflows and outflows. Seepage flow to the CCS does not occur uniformly over the interfaces of the CCS with the surrounding aquifer, and the relative volumes of seepage inflow over the CCS interfaces are shown in Figure 12. It is apparent from Figure 12 that most of the inflow is across the East interface (i.e., the interface facing Biscayne Bay), most of the outflow is across the Bottom interface, relatively lesser volume fluxes occur across of the North, South, and West interfaces, and inflows and outflows occur across all interfaces to varying degrees. The relative seepage contributions from the different faces are important inasmuch as the salinity in the aquifer adjacent to the East interface tends to be at least as high as the salinity in Biscayne Bay, the salinity in the aquifer adjacent to the Bottom interface tends to be on the same order of magnitude as the salinity in the CCS, and lesser salinities occur at the North, South, and West interfaces. The salt contributions from the CCS seepage interfaces are shown in Figure 13. It is apparent that the salt fluxes across the East and Bottom interfaces constitute the predominant components of the salt budget, with influx of salt primarily associated with the East interface and efflux of salt primarily associated with the Bottom interface; keeping in mind that both influx and efflux of salt can occur at these

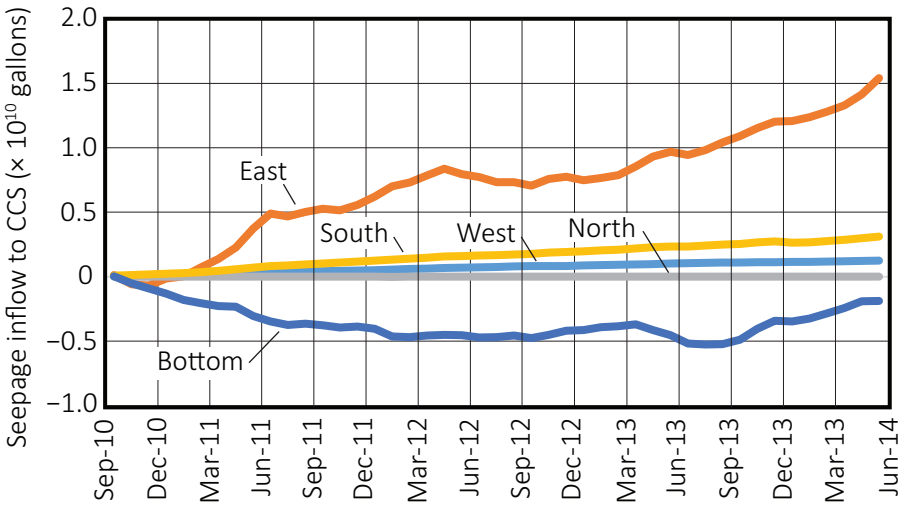

Figure 12: Seepage into CCS from aquifer

interfaces. Lesser but still significant salt influx occurs across the South interface and via ID pumping, with much smaller to negligible salt fluxes across the North and West interfaces. It is apparent from Figure 13 that in the interval September 2013 – May 2014 the flux of salt was primarily and (almost) consistently into the CCS from both the East and Bottom interfaces and, with relatively stable water level and volume in the CCS, this yielded an (almost) consistent increase in the CCS salinity as demonstrated by the measurements shown in Figure 14. Since the seepage influx was driven by the deficit between evaporation and rainfall volumes, it can be concluded that the increase in salinity in the CCS was due directly to the evaporation-rainfall deficit causing contemporaneous influxes of salinity from both the Bottom and East interfaces. Subsequent to the time period covered by Figure 14, salinity in the CCS during 2014 increased to a maximum daily-average value of approximately 99‰. On January 1, 2015, the average salinity in the CCS was 75‰, and by April 26, 2015, salinity levels were over 95‰. From April 27 – 28, 2015, significant rainfall over the CCS reduced the average salinity to 78‰, however, salinities subsequently began rising again in the absence of more rainfall (SFWMD, 2015).

Lessons learned. The results presented in this section clearly demonstrate that the salinity in the CCS can be expected to rise significantly during prolonged periods without rainfall, and that further controls are necessary to ensure that CCS salinity concentrations do not exceed acceptable levels in the future. In October 2015, in response to chloride levels in the Biscayne Aquifer exceeding water-quality standards as a result of the high salinities in the CCS, FPL reached an agreement with Miami-Dade County which includes construction and operation of six wells that would pump water from the CCS into the Boulder Zone of the Floridan Aquifer so as to reduce the salinity in the CCS.

4 Pumping Water from the L-31E Canal into the Cooling Canals

4.1 Pumping Permit and Protocols

In August 2014, SFWMD issued an Emergency Order authorizing the pumping of up to 100 mgd of freshwater from the L-31E Canal to the CCS between August and October 2014, with the primary goal of reducing

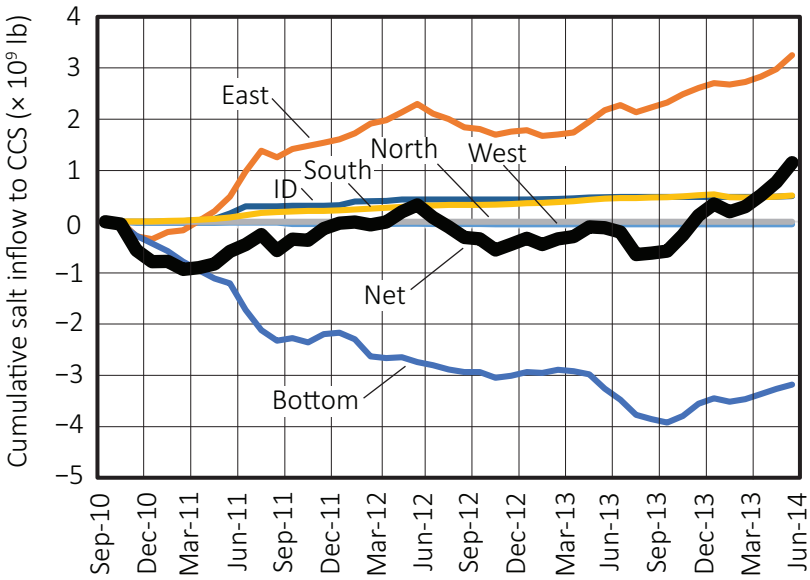

Figure 13: Salt inflow to CCS

the temperature in the CCS. Pursuant to this order, FPL conducted emergency pumping between September 25 and October 15, 2014, and as a result the temperature in the CCS dropped by 6.5°F, the salinity dropped from 87‰ to 75‰, and the algae concentrations reportedly dropped from 1315 cell/L on September 26, 2014 to 68 cell/L on October 27, 2014. After pumping had terminated, algae concentrations again began increasing. Also subsequent to pumping, the temperature in the CCS began to rise again and on April 27, 2015, the intake temperature in the CCS was 98.2°F. A large rainfall event between April 27 and 28, 2015 reduced the temperature in the CCS to 81.3°F, however, by May 17, 2015, the intake temperature had risen to 94.6°F, which was within 10°F of the maximum allowable intake temperature of 104°F. It was primarily on the basis of these conditions that FPL requested a permit to pump additional water from the L-31E Canal into the CCS.

2015 – 2016 Pumping Permit In May 2015, FPL received a permit from the SFWMD to pump up to 100 mgd from the L-31E Canal to the CCS, for the purpose of controlling the temperature in the CCS. Pumping is permitted between June 1 and November 30 in both 2015 and 2016. A limitation stipulated within this permit is that water cannot be withdrawn from the L-31E Canal on any given day until at least 504 acre-ft (2.2×10^7 ft^3) of water has been diverted from the L-31E Canal to Biscayne Bay for purposes of fish and wildlife preservation. Diversion of water from the L-31E Canal to Biscayne Bay occurs through structures S-20F, S-20G, and S-21A, which are located upstream of the CCS withdrawal location (at the "South Pumps") as shown in Figure 15. These three upstream structures open and close based on prescribed water-surface elevations in L-31E Canal at the structure locations, and the open/close stages of these structures are given in Table 3. For example, in the wet-season period of April 30 – October 15 the S-20F, S-20G, and S-21A structures open when the L-31E Canal stage is at or above 0.67 ft NAVD and close when the stage is at or below 0.27 ft NAVD. The cumulative discharges from these structures are monitored daily, to ensure that no pumping from the L-31E Canal into the CCS is allowed until the cumulative discharges from these structures exceed the threshold of 504 acre-ft. The delivery system consists of a northern and southern pump station, where the northern pump station pumps water from the C-103 Basin into the L-31E

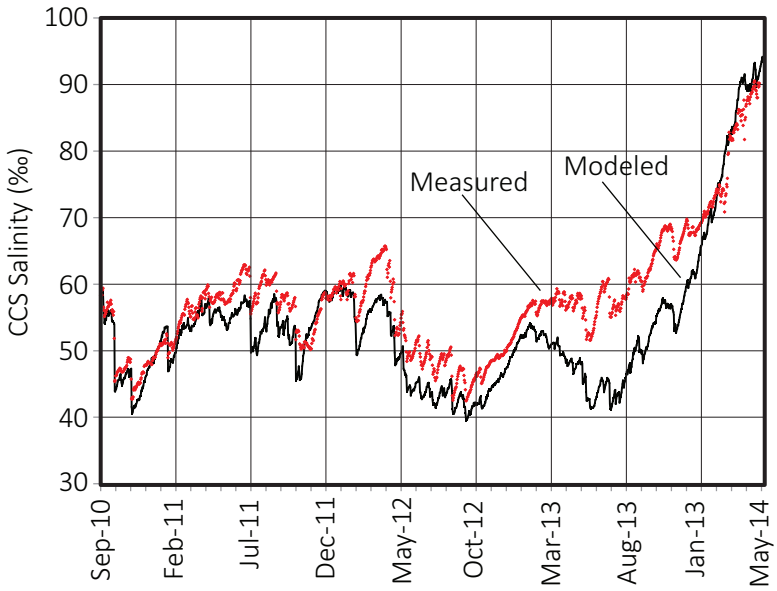

Figure 14: Measured and modeled salinity variations in CCS

Table 3: Gate Operation Rules that Affect L-31E Withdrawals

			L-31E Stage	
			Open	Close
Gate(s)	**Season**	**Period**	(ft NAVD)	(ft NAVD)
S-20F, S-20G, S-21A	Wet	April 30 – October 15	0.67	0.27
S-20F	Dry	October 15 – April 30	−0.13	−0.53
S-20G			0.67	0.27
S-21A			−0.13	−0.53

Canal, and the southern pump station pumps water from the L-31E Canal into the CCS. The operational plan synchronizes northern and southern pumping operations so as to avert dewatering of wetlands between the two pump stations and adjacent to the L-31E Canal. The operational protocol requires that the northern pumps always be started at least five minutes prior to starting the southern pumps, and at the end of each day the southern pumps must be shut down at least five minutes before the northern pumps are shut down. This operational protocol for the pumps ensures that the volume of water pumped daily from the C-103 Basin into the L-31E Canal by the northern pumps exceeds the volume pumped from the L-31E Canal into the CCS by the southern pumps. A particularly important condition of the pumping permit is that FPL is required to monitor the stage in the L-31E Canal between the pumps to ensure that there is no drawdown in the L-31E Canal as a result of the pumping operations. Besides ensuring that there is no L-31N drawdown as a result of pumping, this protocol also ensures that the wetlands adjacent to the L-31N Canal are not dewatered as a result of pumping. Subsequent to beginning of pumping on June 1 2015, the salinity level in the CCS dropped to 70‰, and subsequent large rainfall events have further reduced the CCS salinity to 60‰, according to reports submitted by FPL to the SFWMD.

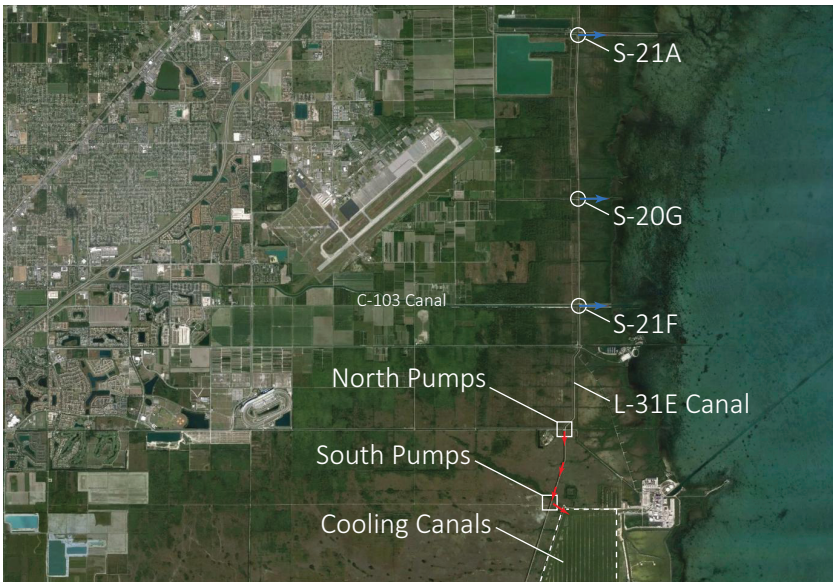

Figure 15: Pumping from L-31E Canal into Cooling-Canal System

4.2 Quantitative Effects

The change in temperature, ΔT, of the water in the CCS resulting from the addition of a volume V_a water at temperature T_a can be approximated using the relation

$$\Delta T = \frac{V_\mathrm{a}}{V_0 + V_\mathrm{a}} \left(T_\mathrm{a} - T_0\right) \tag{9}$$

where V_0 is the initial volume of water in the CCS, and T_0 is the initial temperature of water in the CCS. Equation 9 is a very approximate relationship which assumes that the added water is well mixed over the CCS, and it neglects the differences in density and specific heat between the saline water in the CCS and the fresh water being added. In spite of these shortcomings and in the absence of a detailed heat-balance model of the CCS, Equation 9 can be used to provide a rough estimate of how the temperature in the CCS might react to the addition water from the L-31E Canal. If 100 mgd (= 1.337×10^7 ft^3/d) is added to the CCS which has a volume of 5.746×10^8 ft^3 (assuming an average depth of 2.8 ft) and the added water has a temperature of 75°F, then Equation 9 can be applied using a daily time step to calculate the temperature in the CCS in as a function of number of days of continuous pumping for initial temperatures in the range of 85°F – 100°F. The results of these calculations are shown in Figure 16(a). In a similar manner, the change in salinity, ΔS, in the CCS resulting from the addition water at salinity S_a can be estimated using the approximate relationship

$$\Delta S = \frac{\left(V_\mathrm{a} - V_\mathrm{e}\right)}{V_0 + \left(V_\mathrm{a} - V_\mathrm{e}\right)} \left(S_\mathrm{a} - S_0\right) \tag{10}$$

where S_0 is the initial salinity in the CCS, and V_e is the evaporated volume. Equation 10 is an approximate relationship which assumes that the added water is well mixed over the CCS, and it neglects decreases in salinity that would be caused by rainfall. If 100 mgd is added to the CCS and the rate of evaporation is 39 mgd, then the net rate of freshwater addition to the CCS (i.e., $V_\mathrm{a} - V_\mathrm{e}$) is equal to 61 mgd (= 8.156×10^6 ft^3/d). Using the same CCS volume V_0 that is used for calculating the daily temperature changes, ΔT,

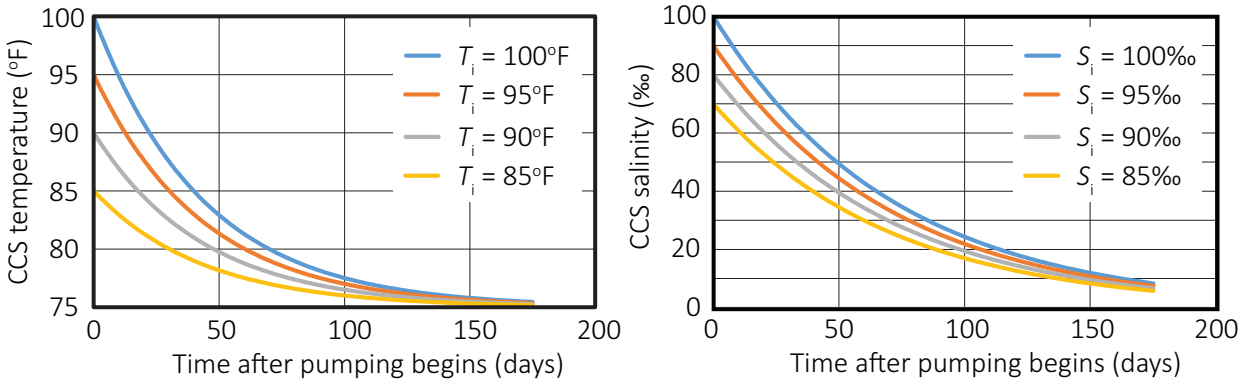

(a) Temperature versus pumping time

(b) Salinity versus pumping time

Figure 16: Approximate effect of pumping 100 mgd on temperature and salinity in CCS

and taking the salinity, S_a of the water pumped from the L-31E Canal equal to zero, Equation 10 can be used to calculate the salinity in the CCS in as a function of number of days of continuous pumping for initial salinities in the range of 70‰ – 100‰ as shown in Figure 16(b). The results in Figure 16 collectively indicate that the sustained addition of 100 mgd from the L-31E Canal to the CCS over continuous times on the order of a week to a month (30 days) would be an effective means of reducing the temperature and salinity in the CCS. The environmental effects on the surrounding environment of pumping water from the L-31E Canal to the CCS are discussed subsequently.

Context. To put a volume flow rate of 100 mgd of fresh water in a societal context, it is noted that 100 mgd is approximately the average daily drinking-water demand of one million people. In the context of the CCS, 100 mgd can be contrasted with the average CCS evaporation rate of around 39 mgd and a long-term average rainfall rate on the CCS of around 21 mgd, where both of these averages are computed over the 9/1/2010 – 5/1/2014 time period. If the CCS were empty and were to be filled by supplying water at 100 mgd, it would take approximately 43 days to fill the CCS. Although 100 mgd is more than twice the evaporation rate, the cooling effect of a unit volume of evaporated water is much greater than the cooling effect of a unit volume of added liquid water. For example, a unit volume of evaporated water would cause a temperature decrease of around 50 times the temperature decrease caused by adding a unit volume of liquid water that is 20°F cooler than the CCS. Therefore, in thermodynamic terms, the addition of 100 mgd of pumped water has approximately the same cooling effect as 2 mgd of evaporated water. With regard to salinity, the salinity reduction resulting from the addition of a unit volume of fresh water exactly compensates for the salinity increase caused by a unit volume of evaporated water. Hence, 39 mgd of added water would neutralize the salinity-increase caused by 39 mgd of evaporated water, with the excess added water causing a reduction in salinity.

4.3 Model Results

The water-balance and salt-balance models used previously by FPL to simulate the pre-uprate salinity dynamics in the CCS were used by FPL to simulate the potential future scenarios with and without the L-31E water inputs in the summer of 2015 and 2016. FPL made minor revisions in the model to incorporate data up through October 2014. The model simulation to predict the response of the CCS to pumping water from the

L-31E Canal started November 1, 2014, and ended November 30, 2016. Two scenarios were simulated at multiple maximum-allowable withdrawal rates, where actual withdrawal rates were predicated on the availability of water in the L-31E Canal after providing 504 acre-ft to Biscayne Bay. Scenario A assumes future conditions that are the same as those observed between November l, 2010 and October 31, 2012; conditions during this time frame reflected normal weather patterns. Scenario B assumes future conditions that are the same as those observed between November 1, 2013 and October 31, 2014; conditions during this time reflected dry weather patterns, and this one-year period was repeated sequentially to produce a two-year predictive simulation. In both scenarios, the conditions observed during the first November (2010, 2013) were repeated to simulate conditions for the last month (November 2016) of the 25-month predictive simulation. Scenario A and Scenario B were each run four times under different pumping scenarios: no pumping, 30 mgd-maximum, 60 mgd-maximum, and 100 mgd-maximum and for a two-year time period. Under all pumping scenarios the simulated CCS water levels increased and simulated CCS salinities decreased relative to the base case of no pumping. Greater changes were observed in response to greater pumping rates. Under all pumping scenarios, the greatest increases in CCS stage occur between June 1 and November 30.

Application of model results. The water-balance and salinity-balance modeling done by FPL in support of the application for the 2015 – 2016 pumping permit focused on the effectiveness of the L-31E pumping on reducing salinity, whereas the primary motivation for pumping from the L-31E Canal is actually to reduce temperature. Elevated temperatures in the CCS will affect power-generation while elevated salinities will not, and there is not a proportional correspondence between reduced salinity and reduced temperature, since temperatures in the CCS depend on a variety of other factors besides the volume of water pumped from the L-31E Canal..

4.4 Environmental Effects

Environmental concerns that have been raised previously by others relate to both the diversion of fresh water from other environmental restoration projects that are currently being serviced by the L-31E Canal, and the utilization of fresh water to dilute hypersaline water, which degrades the quality and utility of the fresh water. Based on available information, it appears that the only environmental projects currently being served directly by the L-31E Canal is the Biscayne Bay fish and wildlife preservation allocation of 504 acre-ft, and the maintenance seasonal water levels in support of adjacent wetlands. The permitted pumping operation will not divert the water volume previously allocated to fish and wildlife preservation, and a pumping protocol will be followed to maintain water levels at their no-pumping levels. With respect to the degradation of fresh water, this degradation will in fact occur, however, the extent of water-quality deterioration and specific deleterious impacts on existing water uses have not to date been identified. Aside from these previously raised concerns, some major additional concerns resulting from pumping up to 100 mgd from the L-31E Canal to the CCS are described below.

4.4.1 Effect of Increased Water-Surface Elevations in the CCS

Pumping water from the L-31E Canal into the CCS will elevate the average water level in the CCS relative to the water level that would exist without pumping. The magnitudes of water-level increases in the CCS were estimated by FPL using the previously developed and calibrated mass balance model of the CCS, and the results of these simulations were submitted to the SFWMD as part of the application for the 2015 – 2016 pumping permit (SFWMD, 2015). Since the water level in the L-31E Canal will be held constant during

pumping operations, the increased water-surface elevations in the CCS are of concern because they will decrease the seaward piezometric-head gradient between the L-31E Canal and the CCS. Furthermore, it is likely that the piezometric-head gradient between the L-31E Canal and the CCS could be reversed from a seaward gradient to a landward gradient. This could produce landward groundwater flow between the CCS and the L-31E Canal, which would likely advect a saline plume from the CCS towards the L-31E Canal. In addition to the aforementioned outcome, elevated water levels in the CCS resulting from pumping 100 mgd from the L-31E Canal will increase the (seaward) piezometric-head gradient between the CCS and Biscayne Bay, resulting in the increased discharge of higher-salinity water from the CCS into the Bay via the Biscayne Aquifer.

Relevant data. To quantify the effect of increased water-surface elevations in the CCS that would occur as a result of pumping, the increased water-surface elevations simulated by FPL were subtracted from historical water-level differences between the L-31E Canal and the CCS to yield possible water-level differences under the 100-mgd pumping scenario. As described previously, two scenarios were modeled, with Scenario A corresponding to "normal" conditions and Scenario B corresponding to "dry" conditions. Each simulation covered two years (2015 and 2016), with pumping in each year from June 1 to November 30. The increases in CCS water-surface elevations over the water-surface elevations that would exist in the CCS without pumping are given in Table 4 for selected dates (about a month apart) during each of these scenarios. The values

Table 4: Estimated Water Level Increases in CCS

Day-Month	**Scenario**	**2015** (ft)	**2016** (ft)
15-Jun	A	0.00	0.23
15-Jul	A	0.00	0.55
15-Aug	A	0.55	0.40
15-Sep	A	0.57	0.40
15-Oct	A	0.50	0.60
15-Nov	A	0.65	0.60
30-Nov	A	0.50	0.45
15-Jun	B	0.00	0.00
15-Jul	B	0.62	0.50
15-Aug	B	0.65	0.70
15-Sep	B	0.15	0.10
15-Oct	B	0.35	0.30
15-Nov	B	0.37	0.55
30-Nov	B	0.50	0.65

given in Table 4 were estimated from graphical plots developed by FPL as part of the permit application. It is apparent from Table 4 that water-level increases in the CCS on the order of 0.5 ft are predicted to occur as a result of pumping water at a rate of 100 mgd from the L-31E Canal into the CCS. These water-level increases can be contrasted with historical differences in the water levels between the L-31E Canal and the CCS for the pre-uprate (June 2011 – May 2012) and post-uprate (June 2013 – May 2014) periods as shown in Table 5, where a positive difference indicates that the water level in the L-31E Canal is higher than the

water level in the CCS. It is apparent from Table 5 that the historical differences between the water levels

Table 5: Historical Water-Level Differences Between L-31E Canal and CCS

Day-Month	**Pre-Uprate** (ft)	**Post-Uprate** (ft)
15-Jun	−0.32	0.46
15-Jul	0.57	0.37
15-Aug	0.80	0.40
15-Sep	0.42	0.48
15-Oct	0.85	0.60
15-Nov	0.51	0.49
30-Nov	0.55	0.45

in the L-31E Canal and the CCS are typically on the same order of magnitude as the expected increases in the CCS water level, and therefore a significant impact on the historical seaward water-level gradient is to be expected. This concern is further amplified when it is considered that a minimum water-level difference of 0.30 ft is required to keep an acceptable seaward water-level gradient and to keep from triggering the interceptor ditch (ID) pumps. If the ID pumps are turned on, this would further elevate the water level in the CCS and further decrease the water-level difference between the L-31E Canal and the CCS.

Demonstration of effects. The increases in the water-surface elevations in the CCS predicted by the FPL mass-balance model can be subtracted from the historical water-level differences between the L-31E Canal and the CCS to estimate the water-level differences between the L-31E Canal and the CCS that are likely to exist as a consequence of pumping a maximum of 100 mgd from the L-31E Canal into the CCS. These expected water-level differences are summarized for the Scenario A (the "normal" condition) in Figure 17(a), and for Scenario B (the "dry" condition) in Figure 17(b). For each historical period (pre-uprate and post-uprate), and for each selected day, three water-level differences are shown: the historical difference (blue), the projected 2015 difference (orange), and the projected 2016 difference (gray). In general, the 2015 and 2016 projected water-level differences are less than the historical differences by the amounts listed in Table 4. Also shown in Figure 17 is the 0.30-ft reference line, which is the threshold water-level difference below which the ID pump system is triggered. It is apparent from Figure 17(a) that under pre-uprate water-level-difference conditions a landward water-level gradient would be created around 15-Sep and 15-Nov on which dates there were previously seaward water-level gradients; the 15-Jun data point is anomalous in that a landward gradient already existed in the historical record. It is further apparent from Figure 17(a) that under post-uprate water-level-difference conditions a landward water-level gradient would be created around 15-Jul, 15-Aug, 15-Sep, 15-Nov, and 30-Nov on which dates there were previously seaward gradients. Under both historical conditions (pre-uprate, post-uprate) shown in Figure 17(a), the difference between the water level in the L-31E Canal and the CCS would fall below the 0.30-ft threshold on all of the dates cited in Figure 17(a). Considering Scenario B (the "dry" condition) shown in Figure 17(b), the results are similar to those shown in Figure 17(a). Under pre-uprate conditions, a landward water-level gradient would be created around 15-Sep and 15-Nov, and under post-uprate water-level-difference conditions a landward water-level gradient would be created around 15-Jul, 15-Aug, 15-Sep, 15-Nov, and 30-Nov. Under both historical conditions, the difference between the water levels in the L-31E Canal and the CCS would fall below the 0.30-ft threshold on all dates cited in Figure 17(b). The results shown in Figure 17 collectively show that

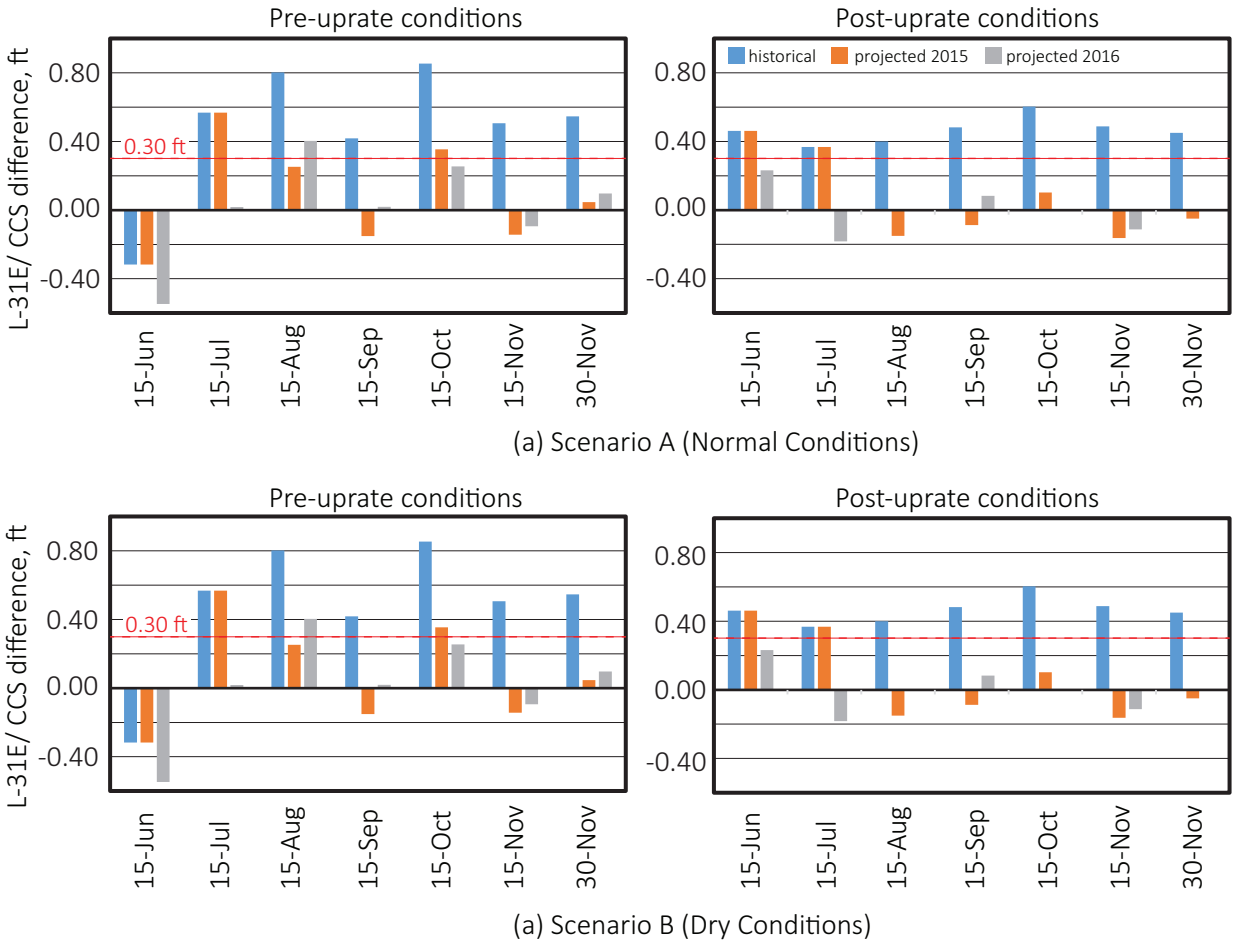

Figure 17: Differences Between L-31E Canal and CCS Water Levels. The historical difference is in blue, the projected 2015 difference is in orange, and the projected 2016 difference is in gray.

there is cause for concern that pumping 100 mgd from the L-31E Canal into the CCS could cause a landward water-level gradient where none previously existed. This concern is further exacerbated when considering that water levels at the northern end of the CCS near the discharge from the power-generating units will be higher that the average water level in the CCS that is used in this analysis, which further decreases the seaward water-level gradient between the L-31E Canal and the CCS. Concern is further heightened when the increased density of water in (and under) the CCS is taken into account, since the difference in equivalent freshwater (piezometric) heads between the L-31E Canal and the CCS is less that the difference in water levels between the L-31E Canal and the CCS. It is actually the difference in equivalent freshwater heads that govern the flow between these bodies of water (e.g., Post et al., 2007). This latter point is particularly important since the difference in freshwater heads between the L-31E Canal and the CCS will increase with depth.

Effect of generating a landward gradient. A landward gradient in the freshwater-equivalent piezometric head between the L-31E Canal and the CCS would advect saline water from the CCS towards the L-31E Canal. Such gradients are likely to be generated under 100-mgd pumping operations. Also, since pumping

would be occurring mostly during the wet season, it is likely that a seaward head gradient would exist (and be maintained) west of the L-31E Canal. As a consequence of a landward gradient in the freshwater-equivalent piezometric head east of the L-31E Canal and a seaward (freshwater) head gradient west of the L-31E Canal, it is possible that a "saline circulation cell" is developed in which water is pumped from the L-31E Canal into the CCS, water seeps out of the CCS and flows through the Biscayne Aquifer back into the L-31E Canal, and then this water is pumped back into the CCS. This circulation cell would increase the salinity in the L-31E Canal, which would degrade the quality of the water in the L-31E Canal and decrease the effectiveness of the pumped water in decreasing the salinity in the CCS.

Historical anecdote. Interestingly, in 1978, engineers from the consulting firm Dames and Moore wrote a report to FPL with a specific section in their report titled "Effects of an Overall Increase in Water Level in the Cooling-Canal System Relative to the Ground Water" (Dames and Moore, 1978). In their report, the engineers at Dames and Moore specifically considered the impact of raising the water level in the CCS by 0.50 ft above the water table in the surrounding aquifer. They concluded that such an occurrence would cause the saltwater interface to move approximately one mile further inland relative to its location prior to the rise in the water level of the CCS.

4.4.2 Suggested Permit Modifications

Based on the concerns described here, along with the supporting analyses provided, it is recommended that the pump-operation protocol associated with the 2015 – 2016 pumping permit be modified to include measurement of water levels in the CCS, and that a threshold water-level difference between the L-31E Canal and the CCS be determined by the SFWMD and added as a controlling factor in pump operations. To ensure that a subsurface circulation cell of saline water does not develop, the salinity of the water in the L-31E Canal should be monitored during pump operations.

5 Conclusions and Recommendations

This brief study consisted of reviewing and summarizing the relevant data and reports relating to the operation of the cooling-canal system (CCS) at the Turkey Point power station, and focusing on three primary issues: (1) the temperature dynamics in the CCS, (2) the salinity dynamics in the CCS, and (3) the impacts and consequences of pumping a maximum of 100 mgd from the L-31E Canal into the CCS.

Temperature dynamics: Temperature dynamics in the CCS are a concern primarily because operation of the power-generating units will be impacted if the temperature of the cooling water at the intake exceeds 104°F. Recent elevated temperatures have come close to exceeding this threshold value. Understanding the temperature dynamics in the CCS is not possible without the development of a heat-balance model of the CCS, and no such model currently exists in the public domain. As part of this study, a preliminary heat-balance model was developed and is described in this report. Using this model to simulate the heat balance in the CCS during the interval 9/1/10 – 12/7/14 showed that there were two distinct periods during which the heat-rejection rate from the power plant remained approximately constant. The first period corresponded to pre-uprate conditions and the second period corresponded to post-uprate conditions. The heat-rejection rate during the second period was found to be significantly greater than the heat-rejection rate during the first period. This finding is not inconsistent with the condition that the post-uprate generating capacity of

the power-generating units served by the CCS is less than the pre-uprate generating capacity, since in the post-uprate generating capacity there is a significant shift from fossil-fuel generation to nuclear-power generation, and nuclear-power units are known to have a much higher heat-rejection rate to cooling water than fossil-fuel generating units. The increased heat-rejection rate in the post-uprate period was manifested in the CCS by increased temperatures. Notably, the average temperature in the discharge zone increased by about 6.3°F (3.5°C) and the average temperature in the intake zone increased by about 4.7°F (2.6°C). Considering that the increased average temperature in the intake zone of the CCS is slightly greater that the increased threshold temperature of 4.0°F (2.2°C) approved by the NRC in 2014, and also considering that supplementary cooling of the CCS was needed in 2014, then caution should be exercised in further increasing power generation beyond 2014 levels without a reliable system to provide additional cooling beyond that currently being provided by the CCS. A power-generation increase would likely lead to a repeat of the need for supplementary cooling that was experienced in 2014. There are also indications that the thermal efficiency of the CCS has decreased in the post-uprate period relative to the thermal efficiency in the pre-uprate period. A sensitivity analysis indicated that increased algae concentrations in the CCS and increased air temperatures are unlikely to have been of sufficient magnitude to cause the elevated temperatures that have been measured in the CCS. In quantitative terms, the additional heating rate in the CCS caused by the presence of high concentrations of algae is estimated to be less than 7% of the heat-rejection rate of the power plant, hence the relatively small effect of algae-induced additional heating. The preliminary findings of this study will need to be followed up by further development of the thermal model supplemented by indirect measurements of heat-rejection rates, and (ideally) flows and temperatures within the CCS, that can be used to calibrate the model within each of the four zones of the CCS. The development of any engineered system to control temperatures in the CCS will need to be done in tandem with thermal-model simulations.

Salinity dynamics: Salinity in the CCS is a concern because increased salinity levels contribute to the increased salinity intrusion into the Biscayne Aquifer. Although an interceptor-ditch salinity-control system is in place, this system is ineffective in controlling salinity intrusion at depth, and so elevated salinities in the CCS remain a problem. This study confirms that long-term salinity increases in the CCS are caused by evaporation rates exceeding rainfall rates. Without any intervention, the trend of increasing salinity would continue into the future. Recent spikes in salinity in the CCS are a normal consequence of a prolonged rainfall deficit and can be expected to recur. Engineered systems that add less-saline water to the CCS to decrease salinity could have an adverse environmental impact caused by the increased water-level elevations in the CCS that these systems create. The effectiveness of an engineered system that pumps saline water from the CCS to deep-well(s) for disposal will depend on the groundwater-flow response in the aquifer surrounding the CCS, the induced salinity-transport dynamics within the aquifer, and the operational protocol of the deep-well injection system. The investigator was made aware through press reports that such a deep-well injection system has been approved for implementation, however, no supporting details were provided by Miami-Dade County to the investigator for further consideration during this study.

Pumping from the L-31E Canal: Pumping of up to 100 mgd from the L-31E Canal into the CCS is permitted between June 1 and November 30 during 2015 and 2016. Mass-balance modeling has shown that this level of pumping will likely raise the average water level in the CCS by around 0.5 ft, and since the historical water-level differences between the L-31E Canal and the CCS are also on the order of 0.5 ft, it is likely that there will be a significant reduction, or even reversal, of the historical seaward water-level gradient that would exist in the absence of pumping. It is even more likely that the water-level difference between the L-31E Canal and the CCS will be reduced below the 0.30-ft threshold that normally triggers the

ID salinity-control system. Model results show a likely reversal of gradient under some circumstances, and a consequence of this reversal could be the advection of a saline plume from the CCS to the L-31E Canal which would cause in increase in the salinity in the L-31E Canal, which is undesirable since the L-31E Canal is regarded as a source of freshwater in its various environmental functions.

Recommended action items. Based on the aforementioned findings, the following action items should be considered:

- Develop a calibrated heat-balance model to simulate the thermal dynamics in the CCS. Essential additional measurements that are required to supplement the calibration of this model are synoptic measurements of volumetric flow rate through the power-generating units, intake temperature, and discharge temperature. Desirable additional measurements include synoptic measurements of the volumetric flow rate and temperature into and out of each CCS zone. The thermal model could be developed to simulate the effects of various supplementary cooling systems to support operation of the CCS.

- Confirm and identify causative factors for the decline in the thermal efficiency of the CCS between the pre-uprate and post-uprate periods.

- Develop a quantitative relationship for estimating algae concentrations as a function of temperature, salinity, and nutrient levels in the CCS. Such a relationship could be derived using data that is already being collected. The developed model could be useful in managing the CCS, since algae concentrations affect the heat balance and possibly the thermal efficiency of the CCS.

- Develop a locally validated relationship between the evaporation rate, water temperature, air temperature, wind speed, salinity, and algae concentrations in the CCS. This is justified since evaporation is the major cooling process in the CCS, and the evaporation model that is currently being used has a high uncertainty level. At present, a constant in the evaporation function is used as a calibration parameter in the salinity-balance model which is not a desirable circumstance given the importance of the evaporation process.

- The operational protocol associated with the 2015 – 2016 permit for transferring up to 100 mgd from the L-31E Canal to the CCS should be modified to include: (1) measurement of water levels in the CCS to preclude a landward equivalent freshwater head gradient being developed, (2) specification of threshold water-level difference between the L-31E Canal and the CCS as a controlling factor in pump operations, and (3) monitoring of the salinity of the water in the L-31E Canal during pump operations to ensure that CCS water is not seeping into the L-31E Canal.

The scope of this study was necessarily limited by the short (120-day) time frame that was available to investigate all of the relevant issues. Follow-on and more detailed investigations will likely lead to a resolution of outstanding issues and the design of robust engineered systems to control the temperature and salinity in the CCS, as well as the extent of salinity intrusion associated with the operation of the CCS. All of these objectives can likely be accomplished with the goal of having sustainable power generation at the Turkey Point station.

References

[1] Adams, E., D. Harleman, G. Jirka, P. Ryan, and K. Stolzenbach. 1975. Heat disposal in the water environment. –. Cambridge, MA : Ralph M. Parsons Laboratory for Water Resources and Hydrodynamics, Massachusetts Institute of Technology.

[2] Brady, D., W. Graves, and J. Geyer. 1969. Surface heat exchange at power plant cooling lakes. Report No. 5. Baltimore, MD : Johns Hopkins University Press.

[3] Brown, L. and T. Barnwell Jr. 1987. The enhanced stream water quality models QUAL2E and QUAL2E-UNCAS: Documentation and Users Manual. – EPA/600/3-87/007. Athens, Georgia : U.S. Environmental Protection Agency.

[4] Byers, H., H. Moses, and P. Harney 1949. Measurement of Rain Temperature. *Journal of Meteorology* 6:51–55.

[5] Chapra, S. 1997. *Surface Water-Quality Modeling*. New York, New York : McGraw-Hill, Inc.

[6] Chin, D. 2013. *Water-Quality Engineering in Natural Systems*. Hoboken, New Jersey : John Wiley & Sons Second edition.

[7] Cogley, J. 1979. The Albedo of Water as a Function of Latitude. *Monthly Weather Review* 107:775–781.

[8] Dames and Moore 1971. Geohydrologic Conditions related to the Construction of Cooling Ponds.

[9] Dames and Moore 1977. Handout, January 1977 FCD/FP&L Semi-Annual Meeting, G-Series Wells Monitoring Program, Turkey Point, Florida Florida Power & Light Company.

[10] Dames and Moore 1978. Salinity Evaluation Turkey Point Cooling Canal System Florida Florida Power & Light Company.

[11] Ecology and Environment, Inc. 2010. Florida Power & Light Company Semi-Annual Report for the Turkey Point Monitoring Project. –. : Prepared for Florida Power & Light Company.

[12] Ecology and Environment, Inc. 2011a. Florida Power & Light Company Semi-Annual Report for the Turkey Point Monitoring Project. –. : Prepared for Florida Power & Light Company.

[13] Ecology and Environment, Inc. 2011b. Florida Power & Light Company Semi-Annual Report for the Turkey Point Monitoring Project. –. : Prepared for Florida Power & Light Company.

[14] Ecology and Environment, Inc. 2012. Pre-Uprate Monitoring Report for Units 3 & 4 Uprate Project. –. : Prepared for Florida Power & Light Company.

[15] Ecology and Environment, Inc. 2012a. Florida Power & Light Company Semi-Annual Report for the Turkey Point Monitoring Project. –. : Prepared for Florida Power & Light Company.

[16] Ecology and Environment, Inc. 2012b. Florida Power & Light Company Semi-Annual Report for the Turkey Point Monitoring Project. –. : Prepared for Florida Power & Light Company.

[17] Ecology and Environment, Inc. 2012c. Comprehensive Pre-Uprate Monitoring Report for the Turkey Point Units 3 & 4 Uprate Project, Section 3. –. : Prepared for Florida Power & Light Company.

[18] Ecology and Environment, Inc. 2013a. Florida Power & Light Company Semi-Annual Report for the Turkey Point Monitoring Project. –. : Prepared for Florida Power & Light Company.

[19] Ecology and Environment, Inc. 2013b. Florida Power & Light Company Semi-Annual Report for the Turkey Point Monitoring Project. –. : Prepared for Florida Power & Light Company.

[20] Ecology and Environment, Inc. 2014. Post-Uprate Monitoring Report for Units 3 & 4 Uprate Project. –. : Prepared for Florida Power & Light Company.

[21] Ecology and Environment, Inc. 2014a. Florida Power & Light Company Semi-Annual Report for the Turkey Point Monitoring Project. –. : Prepared for Florida Power & Light Company.

[22] Ecology and Environment, Inc. 2014b. Florida Power & Light Company Semi-Annual Report for the Turkey Point Monitoring Project. –. : Prepared for Florida Power & Light Company.

[23] Ecology and Environment, Inc. 2015. Florida Power & Light Company Semi-Annual Report for the Turkey Point Monitoring Project. –. : Prepared for Florida Power & Light Company.

[24] Fish, J. and M. Stewart. 1991. Hydrogeology of the surficial aquifer system, Dade County, Florida. Water-Resources Investigations Report No. 90-4108. : United States Geological Survey.

[25] Florida Power and Light Company 2011. Ten year power plant site plan: 2011-2010, Submitted to the Florida Public Service Commission. Miami, FL, April 2011.

[26] Golder Associates 2008. Cooling Canal Data and Analysis Report.

[27] Håkanson, L. and J. Eklund 2010. Relationships Between Chlorophyll, Salinity, Phosphorus, and Nitrogen in Lakes and Marine Areas. *Journal of Coastal Research* 26(3):412–423.

[28] Harbeck, Jr., G. 1955. The Effect of Salinity on Evaporation. Professional Paper No. 272-A. Washington, DC : U.S. Geological Survey.

[29] Howarth, R. and R. Marino 2006. Nitrogen as the limiting nutrient for eutrophication in coastal marine ecosystems: Evolving views over three decades. *Limnology and Oceanography* 51(1, part 2):364–376.

[30] Martin, J. and S. McCutcheon 1998. *Hydrodynamics and Transport for Water Quality Modeling*. Boca Raton, Florida : Lewis Publishers, Inc.

[31] Post, V., H. Kooi, and C. Simmons 2007. Using Hydraulic Head Measurements in Variable-Density Ground Water Flow Analyses. *Ground Water* 45(6):664–671.

[32] Ray L. Lyerly Associates 1973. A Summary Report of the Turkey Point Cooling Canal System.

[33] Ray L. Lyerly Associates 1998. Thermal Performance of the CCS.

[34] Ryan, P. and D. Harleman. 1973. Analytical and experimental study of transient cooling pond behavior. Technical Report No. 161. Cambridge, MA : Ralph M. Parsons Laboratory for Water Resources and Hydrodynamics, Massachusetts Institute of Technology.

[35] Salhorta, A., E. Adams, and D. Harleman 1985. Effect of Salinity and Ionic Composition on Evaporation: Analysis of Dead Sea Evaporation Pans. *Water Resources Research* 21(9):1336–1344.

[36] Sharqawy, M., J. Lienhard V, and S. Zubair 2010. The thermophysical properties of seawater: A review of existing correlations and data. *Desalination and Water Treatment* 16:354380.

[37] South Florida Water Management District 2008. SFWMD Memo to FDEP.

[38] South Florida Water Management District 2015. Emergency Final Order Number 2015-034-DAO-WU. West Palm Beach, Florida.

[39] United States Nuclear Regulatory Commission 2012. Location of projected new nuclear power reactors. Updated March 2012. Accessed: April 2012.

[40] Williams, G. and D. Tomasko 2009. A simple quantitative model to estimate consumptive evaporation impacts of discharged cooling water with minimal data requirements. *Energy and Environment* 20(7):1155–1162.